Versatile synthesis of chiral 6-oxoverdazyl radical ligands – new building blocks for multifunctional molecule-based magnets

Atena B. Solea,[a] Tobie Wohlhauser,[a] Parisa Abbasi,[b] Yvan Mongbanziama,[a] Aurelien Crochet,[c] Katharina M. Fromm,[c] Ghenadie Novitchi,[d] Cyrille Train,[d] Melanie Pilkington*[b] and Olimpia Mamula*[a]

[a.] *Department of Chemistry, University of Applied Sciences Western Switzerland (HES-SO), HEIA-FR, Pérolles 80, CH-1700 Fribourg, Switzerland. Email: olimpia.mamulasteiner@hefr.ch*
[b.] *Department of Chemistry, Brock University, 1812 Sir Isaac Brock Way, St Catharines, Ontario L2S3A1, Canada*
[c.] *Department of Chemistry, University of Fribourg, Ch. du Musee 9, CH-1700 Fribourg, Switzerland*
[d.] *Laboratoire National des Champs Magnétiques Intenses, UPR CNRS 3228, 25, rue des Martyrs, B.P. 166, 38042 Grenoble, France*

Electronic Supplementary Information

S1. Experimental

S1.1 Starting Materials and General Methodology

(–)-myrtenal 98% ee and *(-)*-alpha-pinene 97% ee, purchased from Sigma, were used without further purification. If dry solvents were used, they were stored at RT over molecular sieves 4 Å (8-12 mesh) overnight prior to use. Commercially available chemicals were reagent grade purchased from Sigma Aldrich and used without further purification unless indicated otherwise. Yields reported were for isolated, spectroscopically pure compounds. The Kröhnke salt was synthesized following the reported procedure.[1] *(+)-pinocarvone* was obtained following the method previously described in the literature,[2] using a glass 400ml photo-reactor and a gas-discharge sodium-vapor lamp. ^{i}PrNH-NHBoc,[3] Boc1,[4] 2,4 dimethyl-carbonylhydrazide (**Ha**),[5] 2,4 diisopropyl-carbonylhydrazide (**Hb**)[6] were obtained as described in the literature. When inert conditions were required, the reactions were performed under a N_2 or Ar atmosphere using dried glassware. TLC was carried out on GF254 plates (0.25 mm layer thickness). Flash chromatography was performed using silica gel 60.

Optical rotations were measured on a Anton Paar Modular Circular Polarimeter MCP 100. The measurements were carried out in a quartz vessel (λ = 100 mm) with the sodium D line of a sodium lamp (589 nm).

IR spectra were recorded as solids or oils between 4000 – 400 cm^{-1} on a Bruker ALPHA FTIR. **UV-Vis** spectra were recorded at room temperature on a Perkin Elmer spectrometer Lambda 18 or a Beckman Coulter DU 720 General-Purpose UV-Vis spectrophotometer.

MS spectra were measured with a Bruker FT-MS 4.7T Bio Apex II instrument, while Electrospray Ionization (ESI) measurements were recorded on a Carlo Erba/Kratos EC/ms acquisition system and processed on a SPARC workstation. Samples were introduced through a direct inlet system, with *tris*(perflouroheptyl-S-triazine) as the internal standard. Time-of-Flight mass spectrometry (TOF-MS) measurements were carried out on a micromass LCT – Electrospray Ionization Time-of-Flight mass spectrometer.

NMR ^{1}H NMR spectra were recorded on a Bruker Advance DPX 300 or Bruker Advance AV 400 Digital NMR spectrometer using deuterated solvents with TMS or the residual solvent proton as internal standard ($CDCl_3$ = 7.26 ppm, D_2O=4.79 ppm). Coupling constants are reported in Hz.

Electrochemical studies were performed under nitrogen using a BASi EC-epsilon Autoanalyzer and a standard three-electrode assembly (glassy carbon working, Pt wire auxiliary, and $Ag/AgNO_3$ reference) with 0.1 M NBu_4PF_6 as the supporting electrolyte. Quoted potentials are versus the ferrocene/ferrocenium couple that was used as the internal standard. The scan rates for the cyclic voltammetry were 100 mV/s.

EPR spectra were recorded in solution in quartz tubes on a Bruker Elexsys E580 pulsed spectrometer with a microwave frequency of 9.8705 GHz and 2 Gauss modulation running in continuous wave (*cw*) mode. The EPR data were modelled using the WINSIM simulation software.[7]

DFT calculations: DFT calculations were undertaken on verdazyl radicals **1a** and **2a** based on a geometry-optimized structure using the UB3LYP basis set and 6-311G** functional in Jaguar 9.0.[8]

S1.2 Preparation of Precursor Chiral Aldehydes P1 and P2

The chiral aldehydes precursors **P1** and **P2** were synthesized in three steps (Scheme S1.1) according to the procedure described by Bernhard *et al*.[1] Either (–)-1R-myrtenal or (+)-pinocarvone, drawn from the chiral pool, was reacted with Kröhnke's salt to produce the corresponding 5,6- or 4,5-pinenepyridine furan which was transformed to a methoxycarbonyl group via successive oxidation and esterification reactions. Subsequent reduction with $LiAlH_4$ led to the enantiopure aldehydes **P1** and **P2**.

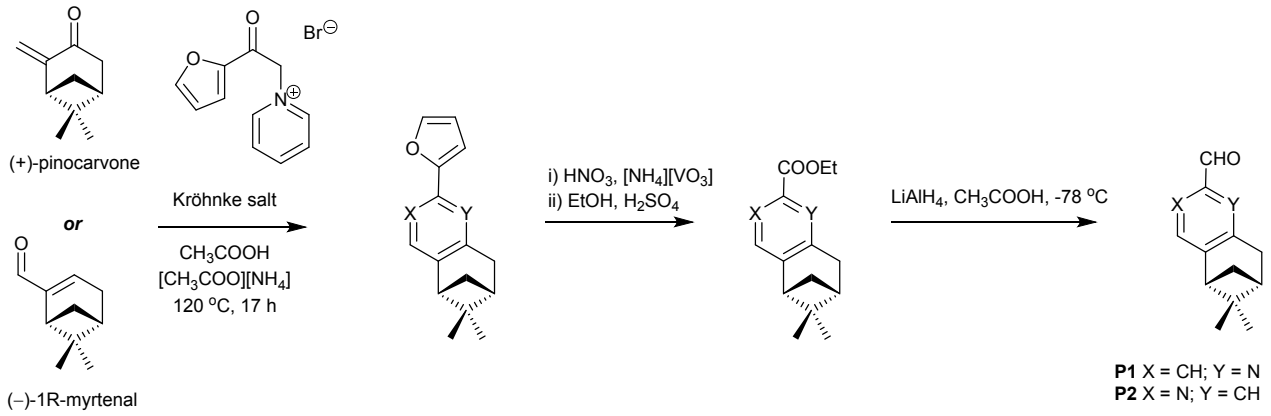

Scheme S1.1 Synthesis of chiral aldehydes **P1** and **P2**.

S1.3 Preparation of Precursor Hydrazides

The 2,4-disubstituted carbohydrazides (**Ha**, **Hb** and **Hc**) were synthesized from the corresponding alkyl hydrazines (Scheme S1.2). The dimethyl derivative (**Ha**) was synthesized in one step according to the literature method.[9] As demonstrated earlier,[6] this straightforward method cannot be applied to hydrazides containing bulkier derivatives (such as **Hb** and **Hc**) due to the smaller difference in nucleophilicity between their primary and secondary amino groups which leads to low regioselectivity and poor yields. Thus, the primary amino group was protected by a Boc group before reaction with phosgene. **Hb** was prepared from coupling *tert*-butyl carbazate together with acetone and subsequent reduction with $NaBH_3CN$.[6] Two different approaches to the diphenyl derivative (**Hc**) have previously been reported. Masuda *et al*.[10] following the previously described *bis*-arylation of carbohydrazide in the presence of CuI in 21% yield. Minor modifications by Matuschek *et al*.[5] led to an improved yield of 37%. Another approach uses 2,4,6-triphenyltetrazinanone which undergoes acid hydrolysis to give the phenyl carbohydrazide.[11] Instead we utilized the route applied to **Hb** to prepare **Hc**. The phenylhydrazine was initially protected with a Boc group,[4] followed by reaction with phosgene, to give the intermediate **Boc2** (Scheme S1.2). The diphenyl derivative **Hc** was readily obtained from deprotection of **Boc2** in a total yield of 41 % for the two-step reaction and required no further purification, simplifying the scale-up.

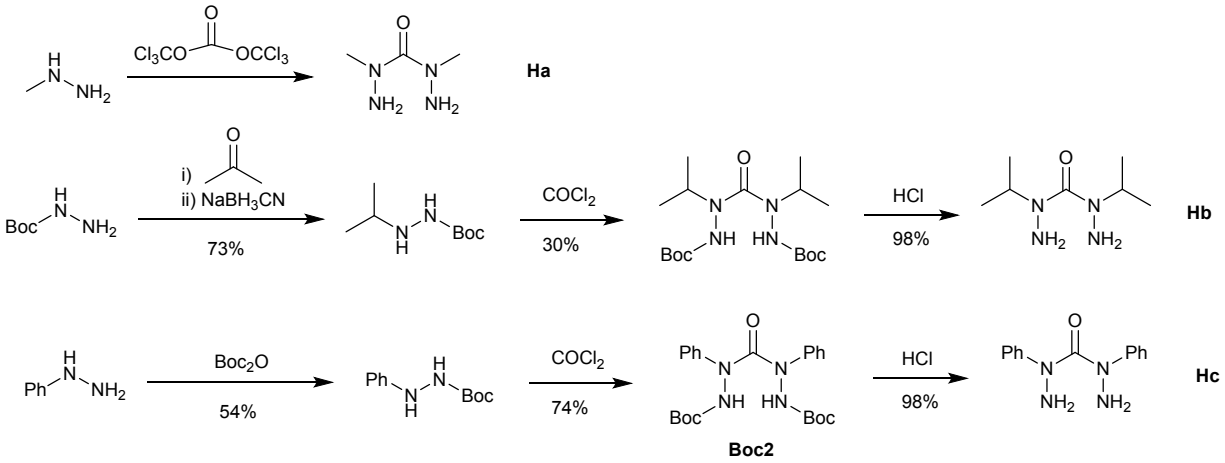

Scheme S1.2 Synthesis of hydrazides **Ha** - **Hc**

Boc protected 2,4-diphenyl-carbonylhydrazide (Boc2)

Boc-phenylhydrazine (19.83g, 95.23mmol, 1eq) was dissolved in dry toluene (100 mL) and dry triethylamine (13.23 ml, 95.23 mmol, 1eq) was added. To this a solution of 20% phosgene in toluene (24.6 ml, 47.61 mmol, 0.5eq) was added dropwise at a rate of less than one drop per second. During the addition, a precipitate of triethylamine hydrochloride was formed. When the addition was complete, the solution was stirred at RT overnight and then filtered. The solvent was evaporated from the filtrate and the resulting solid was dried to give the crude product. This was purified by recrystallization from heptane to give the pure Boc protected 2,4-diphenyl-carbonylhydrazide (**Boc2**) (9.92g, η = 47%) as a light orange solid. **^{1}H NMR** (300 MHz, $CDCl_3$) δ 7.19 (m, 4H, H_{meta}), 6.85 (m, 2H, H_{para}), 6.77 (m, 4H, H_{ortho}) 6.57 (s, 1H), 5.86 (s, 1H), 1.45 (s, 18H). **^{13}C NMR** (75 MHz, $CDCl_3$) δ 156.39, 148.44, 129.13, 120.69, 112.99, 81.17, 28.29. **HRMS (ESI)** *m/z*: $[M+Na]^+$ calcd for $C_{23}H_{30}N_5O$ 465.21084, found 465.21082. **IR**: ῦ = 3350, 3275 (m, NH stretch), 3055, 3000, 2980, 2930 (m, CH stretch), 1700 (s, C=O stretch), 1539, 1495, 1450 (s, CH_3 bending) cm^{-1}.

2,4-diphenyl-carbonylhydrazide·2HCl

Boc2 (443 mg, 1mmol, 1eq) was dissolved in EtOH (8 mL). To this solution, 32% HCl (3 mL) was added dropwise under continuous stirring, during which a mild effervescence was observed. The reaction mixture was stirred at 40°C for 2h. During the course of the reaction a pearly precipitate was formed. After cooling to RT, the solvent was removed under reduced pressure and the solid was further dried under high vacuum affording 0.263 g (83%) of **Hc** as a pearly white solid. **^{1}H NMR** (300 MHz, D_2O) δ 7.41 (dd, $^{3}J_{meta,ortho}$ = 7.8 Hz, $^{3}J_{meta,para}$ = 7.6 Hz, 4H, H_{meta}), 7.15 (t, $^{3}J_{para,meta}$ = 7.6 Hz, 2H, H_{para}), 7.03 (d, $^{3}J_{ortho,meta}$ = 7.8 Hz, 4H, H_{ortho}).

S1.4 Synthesis of the tetrazinanones (T1a-c, T2a-c)

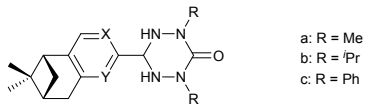

T1: X = CH, Y = N; T2 X = N, Y = CH

Under an inert atmosphere, the corresponding aldehyde (**P1** or **P2**) (1.0 g, 4.96 mmol, 1 eq) was dissolved in MeOH (70 mL). Afterwards, the corresponding carbonylhydrazide (4.96 mmol, 1 eq) was added to the solution. The reaction mixture was refluxed for 24h. After cooling to room temperature, the solvent was removed under reduced pressure to give the corresponding crude products as brown oils. These were purified by flash chromatography on silica gel; For **T1a** and **T2a** the eluent was hexane: EtOAc = 1:1 followed by EtOAc: MeOH = 1:1, for **T1b** the eluent was EtOAc, for **T2b** the preferred eluent was $CHCl_3$: MeOH = 10:1, whereas for **T1c** and **T2c** a mixture 4:1 hexane: EtOAc proved to be the most effective.

(-)-1,5-dimethyl-3-(5,6-pinenepyridine)-tetrazinanone (T1a)

η= 85%. **^{1}H NMR** (300 MHz, $CDCl_3$) δ 7.23 (d, $^{3}J_{3,4}$ = 7.5 Hz, 1H, H3), 7.10 (d, $^{3}J_{4,3}$ = 7.5 Hz, 1H, H4), 5.00 (d,$^{3}J_{NH,1}$ = 10.8 Hz, 2H, NH), 4.80 (dd, $^{3}J_{1,NH}$ = 10.8 Hz, $^{3}J_{1,NHa}$ = 10.8 Hz, 1H, H1), 3.18 (s, 3H, H15), 3.17 (s, 3H, H15a), 3.04 (d, $^{3}J_{10,9}$ = 2.8 Hz, 2H, H10), 2.76 (dd, $^{3}J_{7,11a}$ = 5.7 Hz, $^{3}J_{7,11b}$ = 5.7 Hz, 1H, H7), 2.67 (ddd, $^{2}J_{11b,11a}$ = 9.7 Hz, $^{3}J_{11b,7}$ = 5.8 Hz, $^{3}J_{11b,9}$ = 5.8 Hz, 1H, H11b), 2.36 (m, 1H, H9), 1.40 (s, 3H, H13), 1.20 (d, J = 9.7 Hz, 1H, H11a), 0.60 (s, 3H, H12). **^{13}C NMR** (75 MHz, $CDCl_3$) δ 157.30, 154.46, 150.23, 142.77, 133.82, 120.12, 69.35, 46.33, 39.99, 39.37, 38.06, 38.04, 36.28, 31.75, 25.93, 21.25. **HRMS (ESI)** *m/z*: $[M+H]^+$ calcd for $C_{16}H_{24}N_5O$ 302.19808, found 302.19699. **IR**: ῦ = 3200 (br s, NH), 2900, 2875, 2850 (br m, CH), 1625 (br m, C=O), 1375 (m, CH_3 bending) cm^{-1}. Anal. Calcd for $C_{16}H_{23}N_5O$: C, 63.76; H, 7.69; N, 23.24; Found C, 63.82; H, 7.57; N 23.15. **$[\alpha]_D^{20}$** =-73.6 $deg{\cdot}mL{\cdot}g^{-1}{\cdot}dm^{-1}$ (0.5M in CH_2Cl_2).

(-)-1,5-dimethyl-3-(4,5-pinenepyridine)-tetrazinanone (T2a)

η= 65%. **^{1}H NMR** (300 MHz, $CDCl_3$) δ 8.05 (s, 1H, H6), 7.21 (s, 1H, H3), 4.92 (m, 3H, H1, N2H, N5H), 3.18 (s, 3H, H15), 3.16 (s, 3H, H15a), 2.97 (d, $^{3}J_{10,9}$ = 2.7 Hz, 2H, H10), 2.82 (dd, $^{3}J_{7,11a}$ = 5.8 Hz, $^{3}J_{7,11b}$ = 5.8 Hz, 1H, H7), 2.68 (ddd, $^{2}J_{11b,11a}$ = 9.7 Hz, $^{3}J_{11b,7}$ = 5.8 Hz, $^{3}J_{11b,9}$ = 5.8 Hz, 1H, H11b), 2.29 (m, 1H, H9), 1.39 (s, 3H, H13), 1.14 (d, $^{2}J_{11a,11b}$ = 9.7 Hz, 1H, H11a), 0.60 (s, 3H, H12). **^{13}C NMR** (75 MHz, $CDCl_3$) δ 154.57, 151.49, 146.25, 145.91, 143.61, 123.01, 69.51, 44.52, 40.00, 39.18, 38.20, 38.18, 32.91, 31.76, 26.04, 21.47. **HRMS (ESI)** *m/z*: $[M+H]^+$ calcd for $C_{16}H_{24}N_5O$ 302.19808, found 302.19707. **IR**: ῦ = 3150 (m, NH), 2900, 2875, 2850 (m, CH), 1625 (m, C=O), 1375 (m, CH_3 bending) cm^{-1}. Anal. Calcd for $C_{16}H_{23}N_5O$: C, 63.76; H, 7.69; N, 23.24; Found C, 63.75, H, 7.43; N 23.54. **$[\alpha]_D^{20}$** = -62.9 $deg{\cdot}mL{\cdot}g^{-1}{\cdot}dm^{-1}$ (0.5M in CH_2Cl_2).

(-)-1,5-diisopropyl-3-(5,6-pinenepyridine)-tetrazinanone (T1b)

η= 73%. **^{1}H NMR** (300 MHz, $CDCl_3$) δ 7.20 (d, $^{3}J_{3,4}$ = 7.5 Hz, 1H, H3), 7.03 (d, $^{3}J_{4,3}$ = 7.5 Hz, 1H, H4), 4.68 (hept, J = 6.6 Hz, 2H, H15, H15a), 4.34 (m, 3H, H1, NH), 3.03 (d, $^{3}J_{10,9}$ = 2.6 Hz, 2H, H10), 2.74 (dd, $^{3}J_{7,11a}$ = 5.7 Hz, $^{3}J_{7,11b}$ = 5.7 Hz, 1H, H7), 2.64 (ddd, $^{2}J_{11b,11a}$ = 9.7 Hz, $^{3}J_{11b,7}$ = 5.7 Hz, $^{3}J_{11b,9}$ = 5.7 Hz, 1H, H11b), 2.35 (m, 1H, H9), 1.38 (s, 3H, H13), 1.22 (d, $^{2}J_{11a,11b}$ =9.7 Hz, 1H, H11a), 1.07 (m, 12H, H16, H17, H16a, H17a), 0.62 (s, 3H, H12). **^{13}C NMR** (75 MHz, $CDCl_3$) δ 157.19, 153.60, 151.21, 142.54, 133.84, 120.15, 71.23,

47.66, 47.58, 46.38, 40.08, 39.46, 36.31, 31.77, 26.01, 21.45, 19.50, 19.48, 18.46. **HRMS (ESI)** *m/z*: $[M+H]^+$ calcd for $C_{20}H_{32}N_5O$ 358.26014, found 358.26006. **IR**: ν̃ = 3220 (m, NH), 2960, 2920, 2870 (m, CH), 1670 (s, C=O), 1425, 1385 (s, CH_3 bending) cm^{-1}. Anal. Calcd for $C_{20}H_{31}N_5O$: C, 67.19; H, 8.74; N, 19.59; Found C, 67.22; H, 8.52; N 19.63. $[\alpha]_D^{20}$ = -69.1 deg·mL·g^{-1}·dm^{-1} (0.5M in CH_2Cl_2).

(-)-1,5-diisopropyl-3-(4,5-pinenepyridine)-tetrazinanone (T2b)

η= 59%. **^{1}H NMR** (300 MHz, $CDCl_3$) δ 8.01 (s, 1H, H6), 7.12 (s, 1H, H3), 4.65 (m, 2H, H15, H15a), 4.30 (m, 3H, H1, NH), 2.94 (d, $^3J_{10,9}$ = 2.5 Hz, 2H, H10), 2.77 (dd, $^3J_{7,11a}$ = 5.5 Hz, $^3J_{7,11b}$ = 5.5 Hz, 1H, H7), 2.63 (ddd, $^2J_{11b,11a}$ = 9.8 Hz, $^3J_{11b,7}$ = 5.8 Hz, $^3J_{11b,9}$ = 5.8 Hz, 1H, H11b), 2.23 (m, 1H, H9), 1.35 (s, 3H, H13), 1.13 (d, $^2J_{11a,11b}$ =9.8 Hz, 1H, H11a), 1.05 (m, 12H, H16, H17, H16a, H17a), 0.59 (s, 3H, H12). **^{13}C NMR** (75 MHz, $CDCl_3$) δ 152.34, 151.09, 144.96, 144.61, 142.21, 121.94, 70.00, 46.51, 46.43, 43.24, 38.74, 38.07, 31.70, 30.55, 28.68, 24.88, 20.49, 18.39, 17.38. **HRMS (ESI)** *m/z*: $[M+H]^+$ calcd for $C_{20}H_{32}N_5O$ 358.26014, found 358.26034. **IR**: ν̃ = 3220 (m, NH), 2970, 2920, 2870 (m, CH), 1620 (s, C=O), 1425, 1385 (s, CH_3 bending) cm^{-1}. Anal. Calcd for $C_{20}H_{31}N5O$: C, 67.19; H, 8.74; N, 19.59; Found C, 67.54; H, 8.63; N 19.15. $[\alpha]_D^{20}$ = -54.7 deg·mL·g^{-1}·dm^{-1} (0.5M in CH_2Cl_2).

(-)-1,5-diphenyl-3-(5,6-pinenepyridine)- tetrazinanone (T1c)

η= 45%. **^{1}H NMR** (300 MHz, $CDCl_3$) δ 7.55 (m, 4H), 7.14 (m, 8H), 5.42 (d, $^3J_{N2H,1}$ = 11.2 Hz, 1H, N2H), 5.42 (d, $^3J_{N5H,1}$ = 11.2 Hz, 1H, N5H), 5.12 (dd, $^3J_{1,N2H}$ = 11.2 Hz, $^3J_{1,N5H}$ = 11.2, 1H, H1), 2.93 (d, $^3J_{10,9}$ = 2.4 Hz, 2H, H10), 2.70 (dd, $^3J_{7,11a}$ = 5.5 Hz, $^3J_{7,11b}$ = 5.5 Hz, 1H, H7), 2.55 (m, 1H, H11b), 2.59 (m, 1H, H9), 1.31 (s, 3H, H13), 1.12 (d, $^2J_{11a,11b}$ = 9.7 Hz, 1H, H11a), 0.51 (s, 3H, H12). **^{13}C NMR** (75 MHz, $CDCl_3$) δ: 157.18, 152.21, 150.20, 142.98, 142.49, 142.45, 134.02, 128.38, 128.34, 124.95, 124.81, 123.39, 123.15, 120.33, 71.20, 46.23, 39.89, 39.41, 36.27, 31.78, 25.98, 21.34. **HRMS (ESI)** *m/z*: $[M+H]^+$: calcd. for $C_{26}H_{28}N_5O$ 426.22939, found 426.22901. **IR**: ν̃ = 3241 (b, NH), 3060 (w), 2923(m), 2867 (m, CH), 1653(s, C=O), 1596(s, NH bending), 1491, 1453, 1392, 1353, (s, CH bending, C=C stretch). Anal. Calcd for $C_{26}H_{27}N_5O$: C, 73.39; H, 6.40; N, 16.46; Found C, 73.22; H, 6.63; N 16.67. $[\alpha]_D^{20}$ =-34.7 deg·mL·g^{-1}·dm^{-1} (7.06 mM in CH_2Cl_2).

(-)-1,5-diphenyl-3-(4,5-pinenepyridine)- tetrazinanone (T2c)

η= 50%. **^{1}H NMR** (300 MHz, $CDCl_3$) δ 8.06 (s, 1H), 7.65 (m, 4H), 7.31 (m, 5H), 7.12(m, 2H), 5.51(d, $^3J_{N2H,1}$ = 11.3 Hz, 1H, N2H) 5.43 (d, $^3J_{N5H,1}$ = 11.3 Hz, 1H, N5H), 5.23 (dd, $^3J_{1,N2H}$ = 11.3 Hz, $^3J_{1,N5H}$ = 11.3 Hz, 1H, H1), 3.00 (d, $^3J_{10,9}$ = 2.6 Hz, 2H, H10), 2.83 (dd, $^3J_{7,11a}$ = 5.6 Hz, $^3J_{7,11b}$ = 5.6 Hz, 1H, H7), 2.70 (ddd, $^2J_{11b,11a}$ = 9.7 Hz, $^3J_{11b,7}$ = 5.8 Hz, $^3J_{11b,9}$ = 5.8 Hz, 1H, H11b), 2.32 (m, 1H, H9), 1.41 (s, 3H, H13), 1.09 (d, $^2J_{11a,11b}$ = 9.7 Hz, 1H, H11a), 0.62 (s, 3H, H12). **^{13}C NMR** (75 MHz, $CDCl_3$) δ 152.56, 151.60, 146.30, 146.29, 145.69, 143.74, 142.62, 128.46, 128.42, 125.01, 124.88, 123.34, 123.16, 123.13, 71.48, 44.53, 40.01, 39.22, 32.95, 31.76, 26.05, 21.52. **HRMS (ESI)** *m/z*: $[M+H]^+$: calcd. for $C_{26}H_{28}N_5O$ 426.22939, found 426.22828. **IR**: ν̃ = 3232 (w, NH), 3065, 2922, 2867 (m, CH stretch), 1652(s, C=O), 1596(s, NH bending), 1487, 1454, 1358(s, CH bending, C=C stretch). Anal. Calcd for $C_{26}H_{27}N_5O$: C, 73.39; H, 6.40; N, 16.40; Found C, 73.13; H, 6.34; N 16.17. $[\alpha]_D^{20}$ = -32.7 deg·mL·g^{-1}·dm^{-1} (7.06 mM in CH_2Cl_2).

S1.5 Synthesis of the 6-oxoverdazyl radicals (1a-c and 2a-c)

In a general procedure, the corresponding tetrazinanone (0.235 mmol, 1 eq) was reacted with benzoquinone (38 mg, 0.352 mmol, 1.5 eq), in anhydrous toluene (5 mL) under argon, at reflux, for 1.5h. The solvent was then evaporated under reduced pressure and the residue obtained was purified by column chromatography on silica gel, using a mixture of hexane:EtOAc (4:0.5) as the eluent.

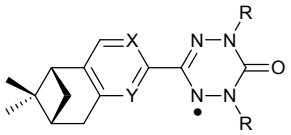

a: R = Me
b: R = ^{i}Pr
c: R = Ph

1: X = CH, Y = N; 2 X = N, Y = CH

(-)-1,5-dimethyl-3-(5,6-pinenepyridine)-oxoverdazyl (1a)

η=42% (29 mg). **HRMS (ESI)** *m/z:* $[M]^+$: calcd. for $C_{16}H_{20}N_5O$ 298.1668, found 298.1663. Anal. Calcd for $C_{16}H_{20}N_5O$: C, 64..41; H, 6.76; N, 23.47; Found C, 64.63; H, 6.55; N 23.78**.** $[\alpha]_D^{20}$ = -26.8 deg·mL·g^{-1}·dm^{-1} (1mM in CH_2Cl_2)

(-)-1,5-diisopropyl-3-(5,6-pinenepyridine)-oxoverdazyl (1b)

η=39% (33 mg). **HRMS (ESI)** *m/z*: $[M+H]^+$: calcd. for $C_{20}H_{29}N_5O$ 355.23721, found 355.23608. Anal. Calcd for $C_{20}H_{28}N_5O$: C, 67.77; H, 7.96; N, 19.76; Found C, 67.39; H, 7.66; N 19.68**.** $[\alpha]_D^{20}$ = -31.1 deg·mL·g^{-1}·dm^{-1} (1mM in CH_2Cl_2)

(-)-1,5-diphenyl-3-(5,6-pinenepyridine)- oxoverdazyl (1c)

η=10% (10 mg). **HRMS (ESI)** *m/z*: $[M + C_6H_4O_2]^+$: calcd. for $C_{32}H_{28}N_5O_3$ 530.21921, found 530.21881. Anal. Calcd for $C_{32}H_{28}N_5O_3$: C, 72.44; H, 5.32; N, 13.20; Found C, 72.21; H, 5.65; N 13.38**.** $[\alpha]_D^{20}$ = -13.3 deg·mL·g^{-1}·dm^{-1} (1mM in CH_2Cl_2)

(-)-1,5-dimethyl-3-(4,5-pinenepyridine)- oxoverdazyl (2a)
η=20% (14 mg). **HRMS (ESI)** *m/z*: $[M]^+$: calcd. for $C_{16}H_{20}N_5O$ 298.1668, found 298.1660. Anal. Calcd for $C_{16}H_{20}N_5O$: C, 64.41; H, 6.76; N, 23.47; Found C, 64.21; H, 6.25; N 23.34**.** $[\alpha]_D^{20}$ = -20.1 deg·mL·g^{-1}·dm^{-1} (c 0.1, DCM).

(-)-1,5-diisopropyl-3-(4,5-pinenepyridine)- oxoverdazyl (2b)
η=14% (12 mg). **HRMS (ESI)** *m/z:* $[M+H]^+$: calcd. for for $C_{20}H_{29}N_5O$ 355.23721, found 355.23687. Anal. Calcd for $C_{20}H_{28}N_5O$: C, 67.77; H, 7.96; N, 19.76; Found C, 67.71; H, 7.66; N 19.75**.** $[\alpha]_D^{20}$ = - 93.2 deg·mL·g^{-1}·dm^{-1} (1mM in CH_2Cl_2)

(-)-1,5-diphenyl-3-(4,5-pinenepyridine)- oxoverdazyl (2c)
η=40% (40 mg). **HRMS (ESI)** *m/z*: $[M+H]^+$: calcd. for $C_{26}H_{25}N_5O$ 423.20591, found 423.20488. Anal. Calcd for $C_{26}H_{24}N_5O$: C, 73.91; H, 5.73; N, 16.58; Found C, 73.87; H, 5.75; N 16.48**.** $[\alpha]_D^{20}$ = - 16.6 deg·mL·g^{-1}·dm^{-1} (1mM in CH_2Cl_2)

S1.6 Preparation of the Cu(II) complex (3b)
Under inert atmosphere, $CuCl_2 \cdot 2H_2O$ (0.168 mmol, 29 mg) in EtOH (1.5 mL) was added over a solution of **2b** (0.168 mmol, 60 mg) in EtOH (1.5 mL). Immediately, the mixture turned purple. The reaction mixture was stirred at room temperature for 30 minutes. Crystallization from the mother mixture at -20°C afforded **3b** as single crystals. Yield: 55 mg, 62%. Anal. Calcd for $C_{20}H_{28}Cl_2CuN_5O$: C, 49.13; H, 5.77; N, 14.32; Found C, 49.45; H, 5.63; N 14.63. **IR**: ṽ = 2922 (s, CH), 1699(s, C=O), 1650 (m, C=N stretch), 1458, 1368, 1287, 1261, 1234, (m, CH bending, C=C stretch, N-N stretch), 433 (w, Cu-N stretch).

S2. Crystallographic Data

Single crystal X-ray structure determination: single crystals of all four compounds were mounted on a cryoloop and data were measured on a STOE IPDS-II diffractometer equipped with an Oxford Cryosystem open flow cryostat[12] using Mo-Kα radiation (λ = 0.71073 Å) at 200 K. Absorption corrections were integrated within the data reduction procedure.[13] The structures were solved and refined using full-matrix least-squares on F^2 with the SHELXL-2014 package.[14] All heavy atoms were refined anisotropically and hydrogen atoms were introduced as fixed contributors when a residual electronic density was observed near their expected positions. All crystal data are presented in Table S1. In the absence of significant anomalous scattering, the absolute structure could not be determined reliably and Friedel pairs were merged and the absolute structure assigned based on the experimentally determined chirality. The final Flack parameters were meaningless because of the high standard deviation from the real value: for **P1** (-0.7(10)), for **P2** (-3(5)) and for **T2b** (1.1(10)). Copies of the data can be obtained on quoting the depository numbers CCDC-1532176 (**P1**), CCDC-1532177 (**P2**), CCDC-1532178 (**T2b**) and CCDC-1811236 (**3b**), (Fax: +44-1223-336-033; E-Mail:deposit@ccdc.cam.ac.uk).

S2.1 Summary of crystallographic data.

Table S2.1 Summary of Crystallographic details for **P1**, **P2**, **T2b** and complex (**3b**)

Compound	P1	P2	T2b	3b
Formula	$C_{13}H_{15}N\,O$	$C_{13}H_{15}NO$	$C_{20}H_{31}N_5O$	$C_{20}H_{28}Cl_2CuN_5O$
FW (g mol^{-1})	201.26	201.26	357.50	488.91
Temperature (K)	200(2)	200(2)	200(2)	200(2)
Crystal System	Monoclinic	Tetragonal	Orthorhombic	Monoclinic
Space Group	$P2_1$	$P4_32_12$	$P2_12_12_1$	$P2_1$
***a* (Å)**	6.5369(4)	7.5168(4)	10.2955(5)	13.0978(9)
***b* (Å)**	7.0071(3)	7.5168(4)	12.3540(10)	11.0063(7)
***c* (Å)**	12.2187(7)	39.316(2)	16.2973(9)	16.8554(14)
***α* (°)**	90	90	90	90
***β* (°)**	100.720(5)	90	90	105.955(6)
***γ* (°)**	90	90	90	90
V (Å^3)	549.91(5)	2221.4(3)	2072.9(2)	2336.2(3)
Z	2	8	4	4
D_C (g. cm^{-3})	1.215	1.204	1.146	1.390
Absorption coefficient (mm^{-1})	0.077	0.076	0.073	1.184
***F*(000)**	216	864	776	1016
Theta range (°)	1.696 to 25.050°	2.072 to 25.156°	2.07 to 24.49	1.256 to 25.196
Index range	-7<=h<=7 -8<=k<=8 -14<=l<=14	-8<=h<=8 -8<=k<=8 -46<=l<=46	-12 ≤ h ≤ 11 -14 ≤ k ≤ 14 -19 ≤ l ≤ 19	-15 ≤ h ≤ 15 -13 ≤ k ≤ 15 -20 ≤ l ≤ 20
Reflections collected	7168	28194	19064	30974
Independent reflections	1944	1977	3694	8315
Data/restraints/parameter	1944 / 1 / 138	1977 / 0 / 140	3694/33/236	8315/97/481
Goodness of fit on F^2 (S)	1.062	1.384	1.013	0.913
Final R_1 (I > 2 ⍰(I))	0.0317	0.0507	0.0673	0.0759
Final wR2 (all data)	0.0891	0.1564	0.1939	0.2174
Largest peak/hole (e$^-$ Å^{-3})	+0.112/-0.130	+0.205/-0.183	+0.189/-0.188	+0.556/-0.459

S.2.2 Molecular structures of P1 and P2

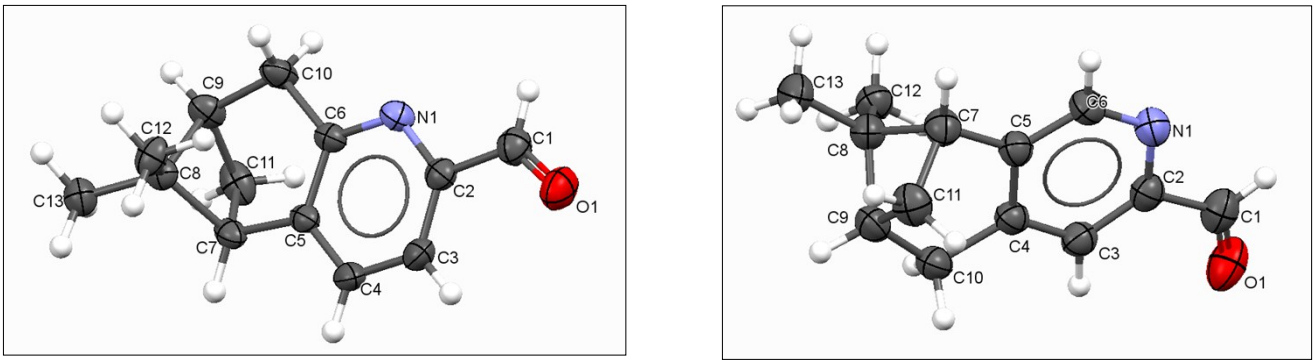

Figure S2.1 Molecular structure of chiral aldehydes, **P1** (left) and **P2** (right) with appropriate labelling scheme. Thermal ellipsoids are plotted at 50%.

Table S2.1 Selected geometric parameters for **P1** (Å, °)

Bond	Length (Å)	Bond	Length (Å)
C1—O1	1.203 (3)	C6—C10	1.504 (2)
C1—C2	1.473 (3)	C7—C11	1.543 (3)
C2—N1	1.344 (3)	C7—C8	1.560 (3)
C2—C3	1.375 (3)	C8—C12	1.513 (3)
C3—C4	1.381 (3)	C8—C13	1.526 (2)
C4—C5	1.377 (3)	C8—C9	1.559 (3)
C5—C6	1.407 (2)	C9—C10	1.526 (3)
C5—C7	1.498 (3)	C9—C11	1.534 (4)
C6—N1	1.326 (2)		
Bond	**Angle (°)**	**Bond**	**Angle (°)**
O1—C1—C2	125.4 (2)	C11—C7—C8	87.11 (16)
N1—C2—C3	123.51 (18)	C12—C8—C13	108.80 (17)
N1—C2—C1	115.15 (17)	C12—C8—C9	118.90 (17)
C3—C2—C1	121.33 (18)	C13—C8—C9	111.62 (15)
C2—C3—C4	118.48 (19)	C12—C8—C7	118.51 (16)
C5—C4—C3	119.47 (17)	C13—C8—C7	112.38 (15)
C4—C5—C6	117.98 (17)	C9—C8—C7	85.01 (15)
C4—C5—C7	125.65 (16)	C10—C9—C11	108.30 (19)
C6—C5—C7	116.37 (17)	C10—C9—C8	112.07 (16)
N1—C6—C5	122.96 (16)	C11—C9—C8	87.45 (15)
N1—C6—C10	119.10 (14)	C6—C10—C9	110.89 (15)
C5—C6—C10	117.94 (16)	C9—C11—C7	86.42 (16)
C5—C7—C11	107.30 (15)	C6—N1—C2	117.55 (15)
C5—C7—C8	109.93 (14)		

Table S2.2 Selected geometric parameters for **P2** (Å, °)

Bond	Length (Å)	Bond	Length (Å)
C1—O1	1.199 (5)	C6—N1	1.329 (5)
C1—C2	1.468 (5)	C7—C11	1.551 (5)
C2—N1	1.344 (5)	C7—C8	1.568 (5)
C2—C3	1.380 (5)	C8—C12	1.514 (6)
C3—C4	1.379 (5)	C8—C13	1.522 (5)
C4—C5	1.404 (5)	C8—C9	1.560 (5)
C4—C10	1.506 (5)	C9—C10	1.519 (5)
C5—C6	1.386 (5)	C9—C11	1.542 (6)
C5—C7	1.486 (5)		
Bond	**Angle (°)**	**Bond**	**Angle (°)**
O1—C1—C2	125.4 (4)	C11—C7—C8	87.3 (3)
N1—C2—C3	123.5 (3)	C12—C8—C13	109.1 (3)
N1—C2—C1	114.2 (3)	C12—C8—C9	118.3 (3)
C3—C2—C1	122.3 (4)	C13—C8—C9	112.4 (3)
C4—C3—C2	119.9 (3)	C12—C8—C7	119.3 (3)
C3—C4—C5	117.4 (3)	C13—C8—C7	111.1 (3)
C3—C4—C10	124.8 (3)	C9—C8—C7	84.9 (2)
C5—C4—C10	117.8 (3)	C10—C9—C11	108.7 (3)
C6—C5—C4	118.3 (3)	C10—C9—C8	111.3 (3)
C6—C5—C7	125.0 (3)	C11—C9—C8	88.0 (3)
C4—C5—C7	116.7 (3)	C4—C10—C9	110.9 (3)
N1—C6—C5	124.6 (3)	C9—C11—C7	86.0 (3)
C5—C7—C11	106.8 (3)	C6—N1—C2	116.4 (3)
C5—C7—C8	110.2 (3)		

Table S2.3 Selected geometric parameters for **T2b** (Å, °)

Bond	Length (Å)	Bond	Length (Å)
C1—N2	1.440 (9)	C8—C9	1.552 (11)
C1—N5	1.442 (8)	C9—C11	1.521 (11)
C1—C2	1.509 (7)	C9—C10	1.529 (9)
C2—N1	1.340 (7)	C14—O1	1.238 (6)
C2—C3	1.366 (7)	C14—N3	1.362 (9)
C3—C4	1.383 (8)	C14—N4	1.373 (8)
C4—C5	1.391 (7)	C15—N4	1.466 (8)
C4—C10	1.519 (8)	C15—C16	1.498 (10)
C5—C6	1.371 (7)	C15—C17	1.526 (10)
C5—C7	1.491 (7)	C15A—N3	1.467 (9)
C6—N1	1.341 (7)	C15A—C16A	1.506 (10)
C7—C11	1.542 (11)	C15A—C17A	1.521 (10)
C7—C8	1.566 (9)	N2—N3	1.440 (7)
C8—C12	1.509 (12)	N4—N5	1.430 (7)
C8—C13	1.543 (9)		

Bond	Angle (°)	Bond	Angle (°)
N2—C1—N5	114.0 (5)	C11—C9—C10	109.3 (6)
N2—C1—C2	109.6 (5)	C11—C9—C8	88.3 (6)
N5—C1—C2	108.0 (5)	C10—C9—C8	111.1 (6)
N1—C2—C3	123.3 (5)	C4—C10—C9	110.3 (5)
N1—C2—C1	114.6 (5)	C9—C11—C7	86.3 (7)
C3—C2—C1	122.1 (5)	O1—C14—N3	120.2 (7)
C2—C3—C4	119.5 (5)	O1—C14—N4	120.9 (7)
C3—C4—C5	118.5 (5)	N3—C14—N4	118.8 (5)
C3—C4—C10	123.7 (5)	N4—C15—C16	109.3 (6)
C5—C4—C10	117.7 (5)	N4—C15—C17	111.1 (6)
C6—C5—C4	117.5 (5)	C16—C15—C17	113.7 (7)
C6—C5—C7	125.7 (5)	N3—C15A—C16A	110.6 (6)
C4—C5—C7	116.8 (5)	N3—C15A—C17A	111.9 (6)
N1—C6—C5	124.9 (5)	C16A—C15A—C17A	110.4 (7)
C5—C7—C11	107.0 (6)	C2—N1—C6	116.2 (4)
C5—C7—C8	110.3 (5)	C1—N2—N3	110.1 (5)
C11—C7—C8	87.1 (6)	C14—N3—N2	121.8 (5)
C12—C8—C13	110.4 (8)	C14—N3—C15A	119.0 (6)
C12—C8—C9	119.4 (7)	N2—N3—C15A	112.3 (6)
C13—C8—C9	111.1 (7)	C14—N4—N5	119.7 (5)
C12—C8—C7	118.6 (6)	C14—N4—C15	119.4 (5)
C13—C8—C7	110.6 (6)	N5—N4—C15	113.2 (6)
C9—C8—C7	84.4 (6)	N4—N5—C1	111.4 (5)

Table S2.4 Selected geometric parameters for **3b** (Å, °)

Bond	Length (Å)	Bond	Length (Å)
C1—N5	1.32 (3)	C24—C25	1.43 (4)
C1—N2	1.38 (3)	C24—C30	1.51 (4)
C1—C2	1.48 (4)	C25—C26	1.37 (4)
C2—N1	1.30 (3)	C25—C27	1.51 (3)
C2—C3	1.44 (4)	C26—N6	1.31 (4)
C3—C4	1.38 (4)	C27—C31	1.56 (3)
C4—C5	1.39 (3)	C27—C28	1.59 (3)
C4—C10	1.52 (4)	C28—C29	1.51 (3)
C5—C6	1.38 (3)	C28—C32	1.53 (3)
C5—C7	1.50 (3)	C28—C33	1.54 (3)
C6—N1	1.40 (4)	C29—C30	1.56 (3)
C7—C8	1.54 (3)	C29—C31	1.57 (4)
C7—C11	1.60 (3)	C34—O2	1.21 (3)
C8—C12	1.52 (4)	C34—N9	1.35 (4)
C8—C13	1.54 (3)	C34—N8	1.44 (4)
C8—C9	1.58 (3)	C35—N9	1.44 (3)
C9—C10	1.51 (3)	C35—C37	1.51 (3)

C9—C11	1.52 (4)	C35—C36	1.54 (3)
C14—O1	1.23 (3)	C35A—N8	1.48 (4)
C14—N3	1.34 (4)	C35A—C37A	1.51 (4)
C14—N4	1.41 (4)	C35A—C36A	1.52 (4)
C15—N4	1.50 (3)	Cl1—Cu1	2.204 (9)
C15—C16	1.51 (4)	Cl2—Cu1	2.210 (9)
C15—C17	1.54 (3)	Cl3—Cu2	2.226 (9)
C15A—C17A	1.48 (4)	Cl4—Cu2	2.186 (9)
C15A—N3	1.48 (3)	Cu1—N2	1.96 (2)
C15A—C16A	1.58 (4)	Cu1—N1	2.00 (2)
C21—N10	1.29 (3)	Cu2—N7	1.97 (2)
C21—N7	1.36 (3)	Cu2—N6	1.98 (2)
C21—C22	1.52 (4)	N2—N3	1.36 (3)
C22—C23	1.32 (4)	N4—N5	1.32 (3)
C22—N6	1.37 (3)	N7—N8	1.36 (3)
C23—C24	1.36 (4)	N9—N10	1.38 (3)

Bond	**Angle (°)**	**Bond**	**Angle (°)**
N5—C1—N2	127 (2)	C32—C28—C33	110 (2)
N5—C1—C2	119 (3)	C29—C28—C27	85.7 (17)
N2—C1—C2	114 (3)	C32—C28—C27	115 (2)
N1—C2—C3	125 (3)	C33—C28—C27	109.6 (18)
N1—C2—C1	111 (3)	C28—C29—C30	111.8 (18)
C3—C2—C1	124 (3)	C28—C29—C31	90 (2)
C4—C3—C2	116 (3)	C30—C29—C31	107 (2)
C3—C4—C5	120 (3)	C24—C30—C29	111 (2)
C3—C4—C10	119 (2)	C27—C31—C29	84.2 (18)
C5—C4—C10	121 (3)	O2—C34—N9	127 (3)
C6—C5—C4	121 (2)	O2—C34—N8	118 (3)
C6—C5—C7	123 (2)	N9—C34—N8	115 (3)
C4—C5—C7	116 (2)	N9—C35—C37	110 (2)
C5—C6—N1	120 (2)	N9—C35—C36	105 (2)
C5—C7—C8	110.3 (18)	C37—C35—C36	113 (3)
C5—C7—C11	106.9 (18)	N8—C35A—C37A	111 (2)
C8—C7—C11	84.7 (18)	N8—C35A—C36A	110 (2)
C12—C8—C13	106 (2)	C37A—C35A—C36A	111 (2)
C12—C8—C7	118 (2)	N2—Cu1—N1	80.8 (8)
C13—C8—C7	114 (2)	N2—Cu1—Cl1	93.3 (7)
C12—C8—C9	118 (2)	N1—Cu1—Cl1	129.9 (8)
C13—C8—C9	114.0 (18)	N2—Cu1—Cl2	142.8 (7)
C7—C8—C9	86.6 (16)	N1—Cu1—Cl2	102.5 (7)
C10—C9—C11	113 (2)	Cl1—Cu1—Cl2	110.7 (3)
C10—C9—C8	110.9 (18)	N7—Cu2—N6	81.9 (10)
C11—C9—C8	86.3 (18)	N7—Cu2—Cl4	143.6 (6)
C9—C11—C7	86.9 (19)	N6—Cu2—Cl4	98.2 (8)
C9—C10—C4	109 (2)	N7—Cu2—Cl3	94.1 (7)

O1—C14—N3	126 (3)	N6—Cu2—Cl3	133.2 (7)
O1—C14—N4	118 (3)	Cl4—Cu2—Cl3	110.8 (3)
N3—C14—N4	115 (3)	C2—N1—C6	118 (3)
N4—C15—C16	108 (2)	C2—N1—Cu1	114 (2)
N4—C15—C17	110 (2)	C6—N1—Cu1	127.9 (18)
C16—C15—C17	114 (3)	N3—N2—C1	112 (2)
C17A—C15A—N3	115 (2)	N3—N2—Cu1	126.1 (17)
C17A—C15A—C16A	109 (3)	C1—N2—Cu1	105.3 (17)
N3—C15A—C16A	106 (2)	C14—N3—N2	125 (2)
N10—C21—N7	131 (3)	C14—N3—C15A	118 (2)
N10—C21—C22	118 (3)	N2—N3—C15A	117 (2)
N7—C21—C22	110 (3)	N5—N4—C14	122 (3)
C23—C22—N6	123 (3)	N5—N4—C15	115 (2)
C23—C22—C21	123 (3)	C14—N4—C15	123 (2)
N6—C22—C21	113 (3)	N4—N5—C1	117 (2)
C22—C23—C24	121 (3)	C26—N6—C22	117 (3)
C23—C24—C25	117 (3)	C26—N6—Cu2	130 (2)
C23—C24—C30	126 (3)	C22—N6—Cu2	112 (2)
C25—C24—C30	117 (3)	N8—N7—C21	113 (2)
C26—C25—C24	118 (3)	N8—N7—Cu2	124 (2)
C26—C25—C27	125 (2)	C21—N7—Cu2	109.1 (18)
C24—C25—C27	116 (3)	N7—N8—C34	122 (3)
N6—C26—C25	124 (3)	N7—N8—C35A	121 (2)
C25—C27—C31	106 (2)	C34—N8—C35A	117 (2)
C25—C27—C28	110.3 (17)	C34—N9—N10	125 (3)
C31—C27—C28	87 (2)	C34—N9—C35	117 (2)
C29—C28—C32	121 (2)	N10—N9—C35	117 (2)
C29—C28—C33	113.9 (19)	C21—N10—N9	113 (2)

S3 Selective analytical data

S3.1 ^{1}H NMR data

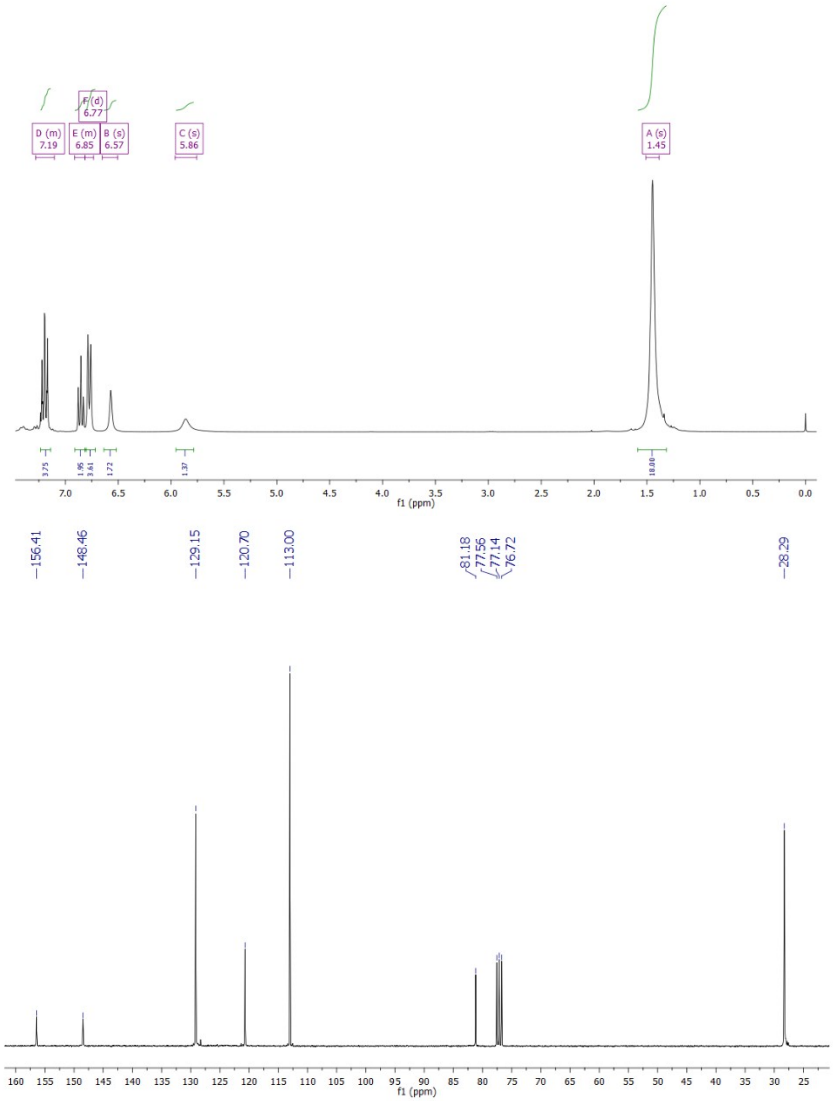

Figure S3.1.1. ^{1}H NMR (top) and ^{13}C-NMR (bottom) of **Boc2** in $CDCl_3$.

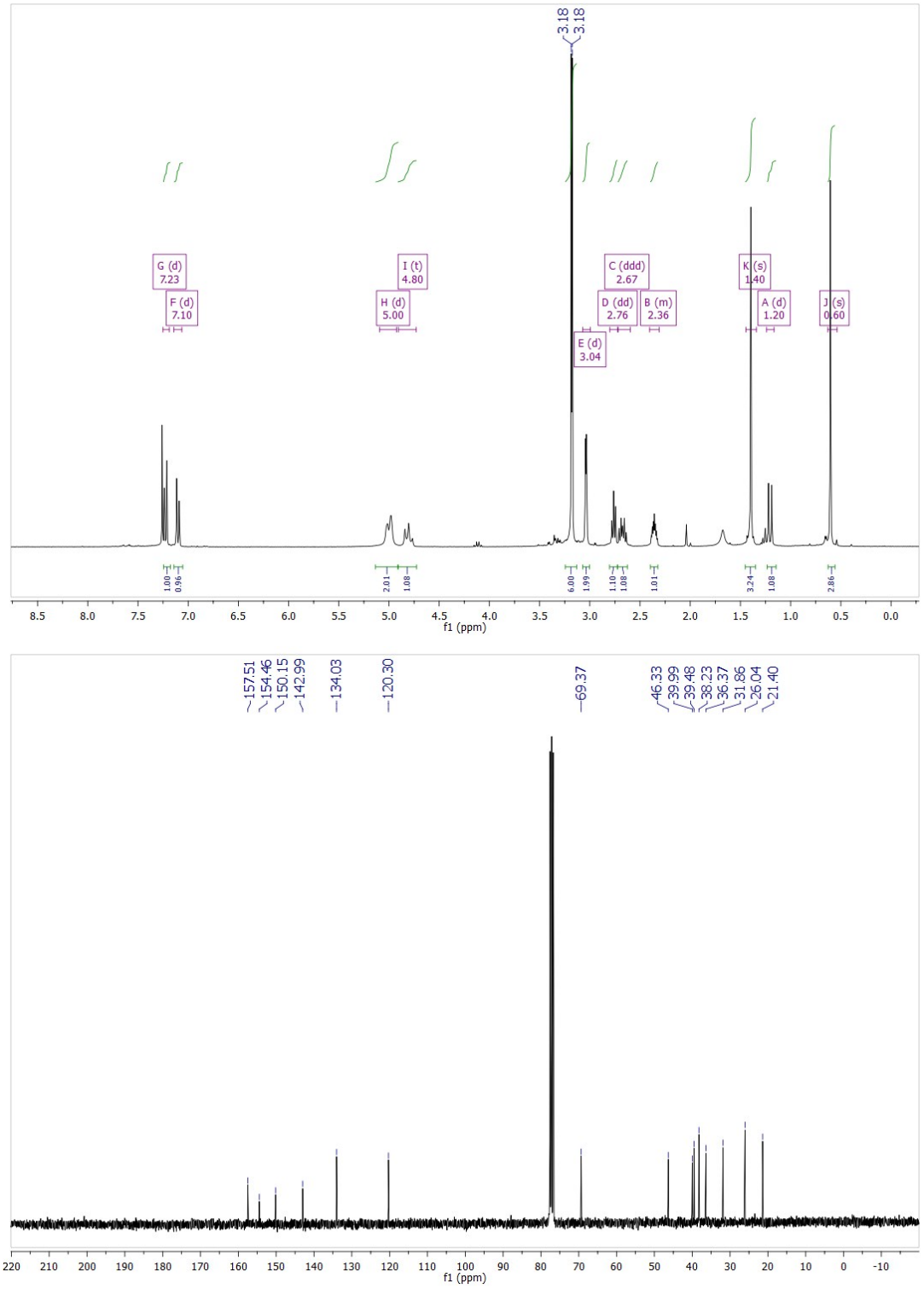

Figure S3.1.2. ^{1}H NMR (top) and ^{13}C-NMR (bottom) of **T1a** in $CDCl_3$.

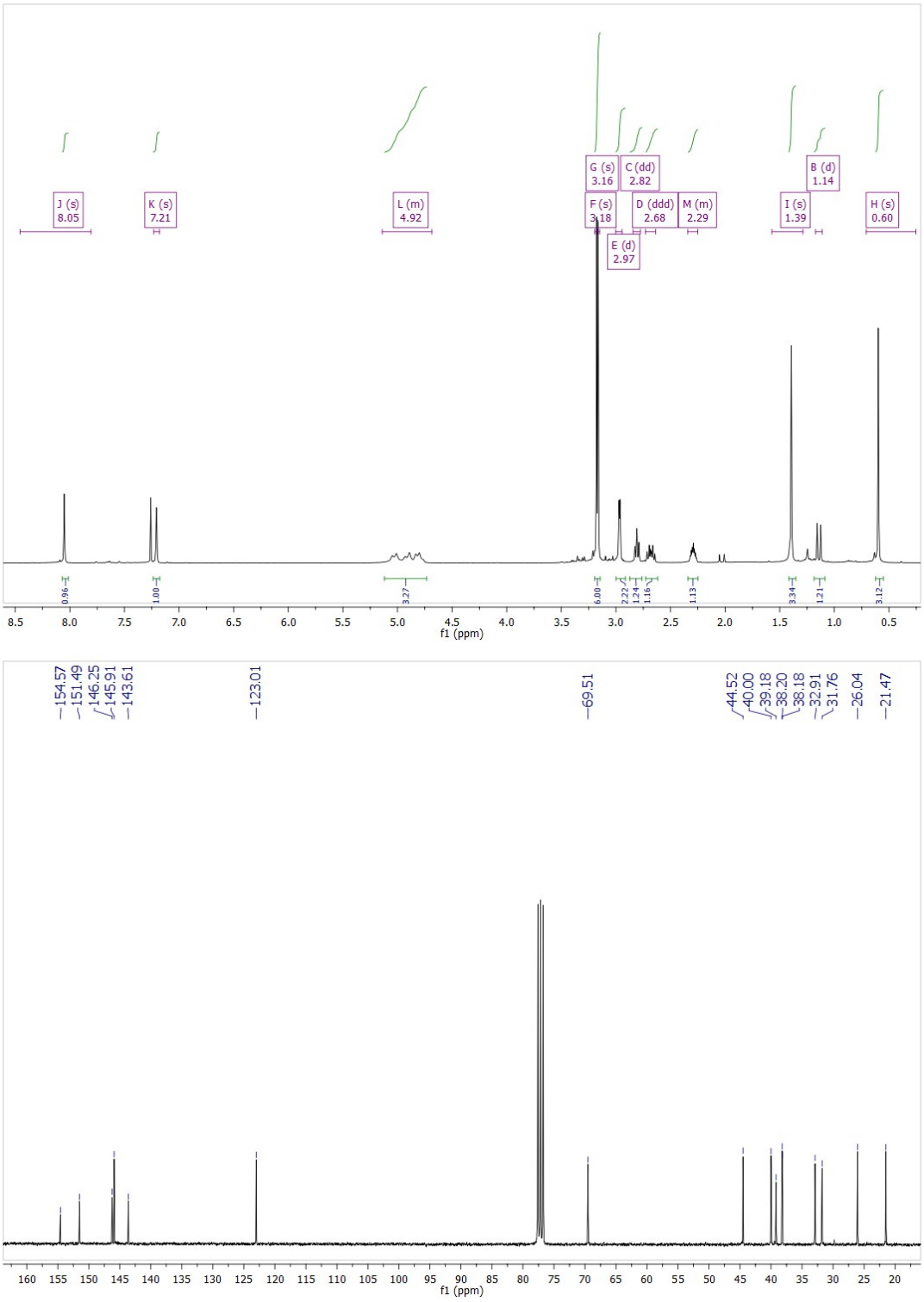

Figure S3.1.3. ^{1}H NMR (top) and ^{13}C-NMR (bottom) of **T2a** in $CDCl_3$.

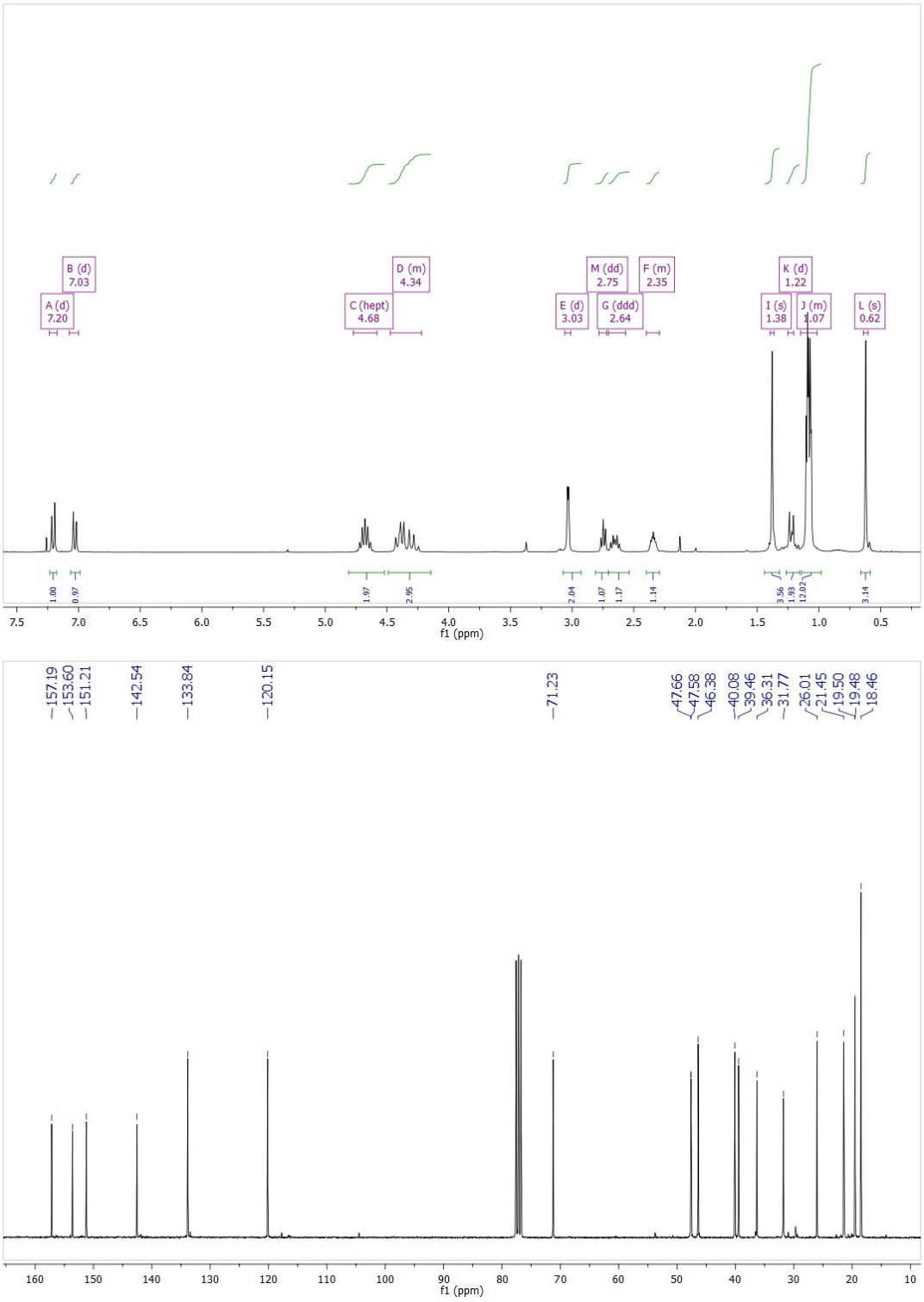

Figure S3.1.4. ^{1}H NMR (top) and ^{13}C-NMR (bottom) of **T1b** in $CDCl_3$.

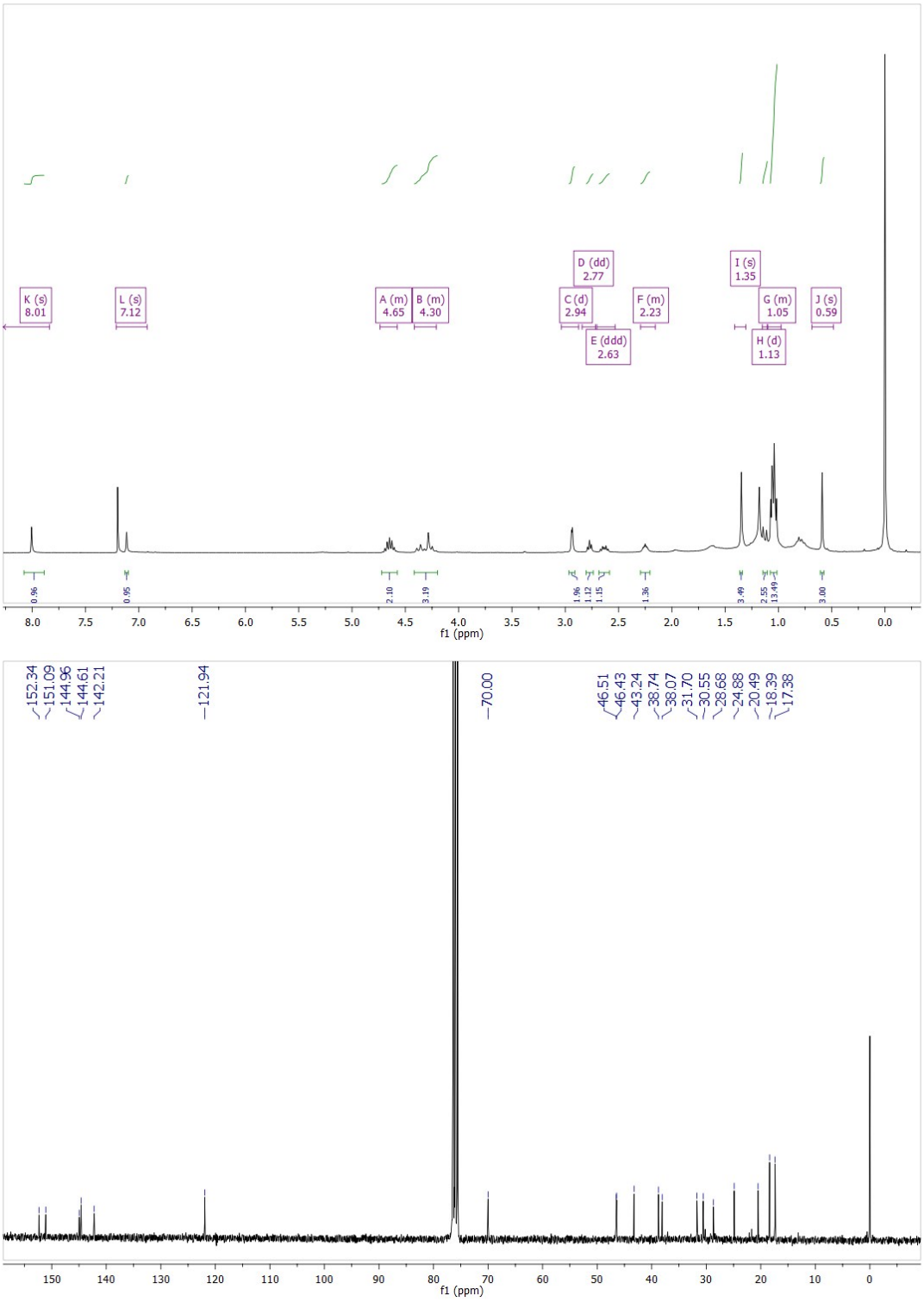

Figure S3.1.5. ^{1}H NMR (top) and ^{13}C-NMR (bottom) of **T2b** in $CDCl_3$.

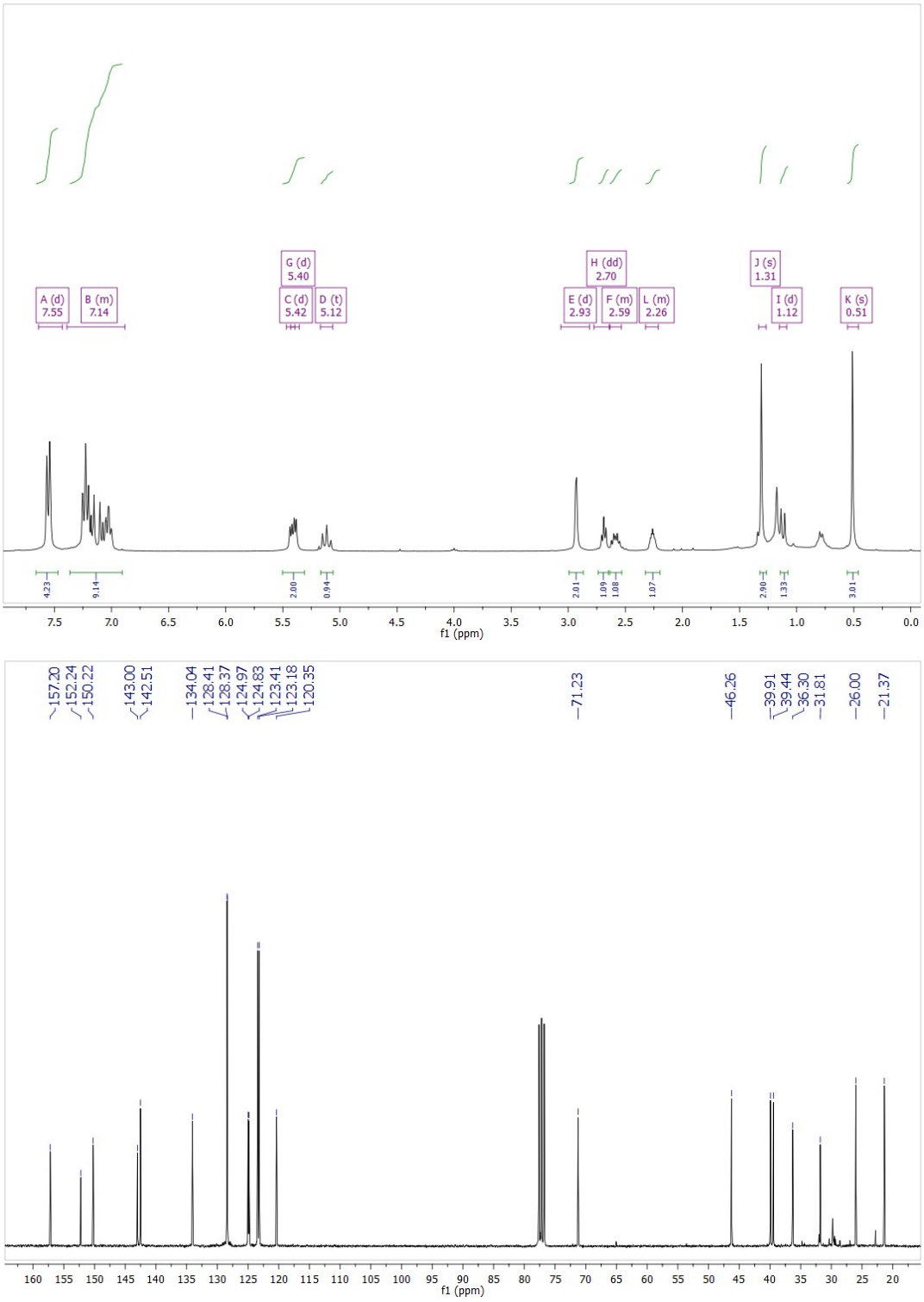

Figure S3.1.6. ^{1}H NMR (top) and ^{13}C-NMR (bottom) of **T1c** in $CDCl_3$.

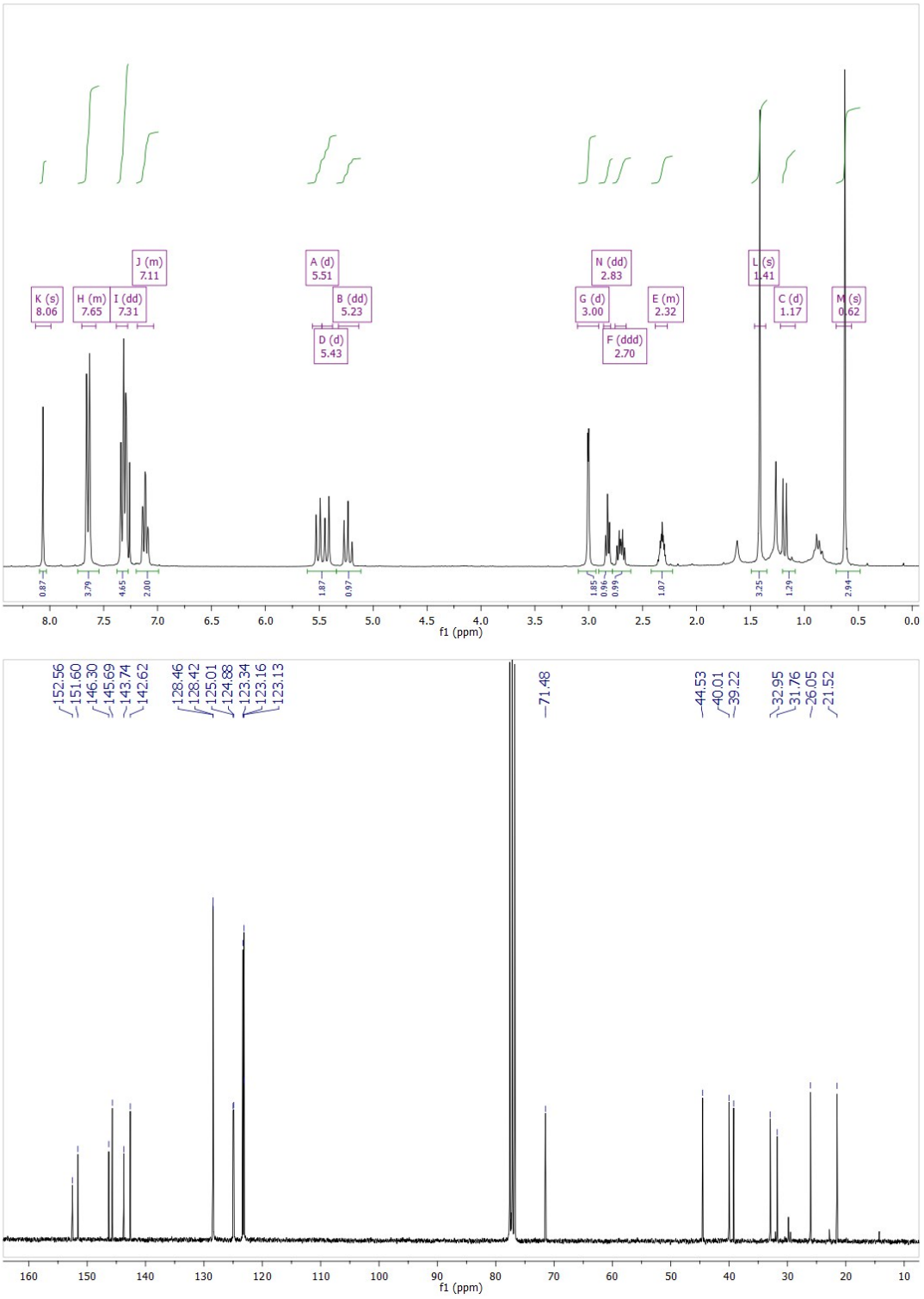

Figure S3.1.7. ^{1}H NMR (top) and ^{13}C-NMR (bottom) of **T2c** in $CDCl_3$.

S 3.2 IR Spectroscopy Data

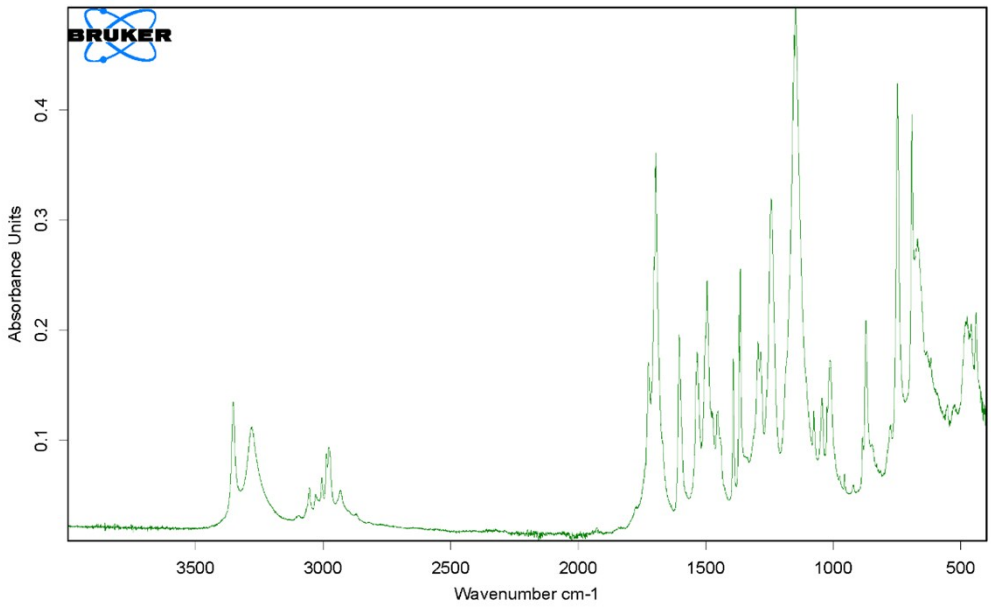

Figure S3.2.1. IR data for **Boc2**

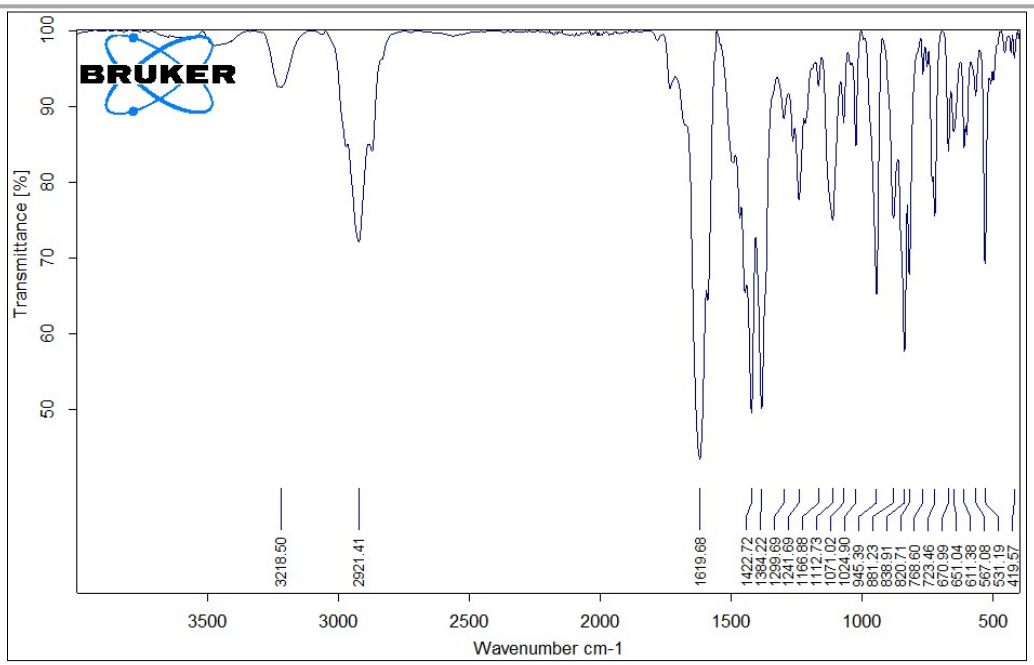

Figure S3.2.2. IR data for tetrazinanone **T1a**

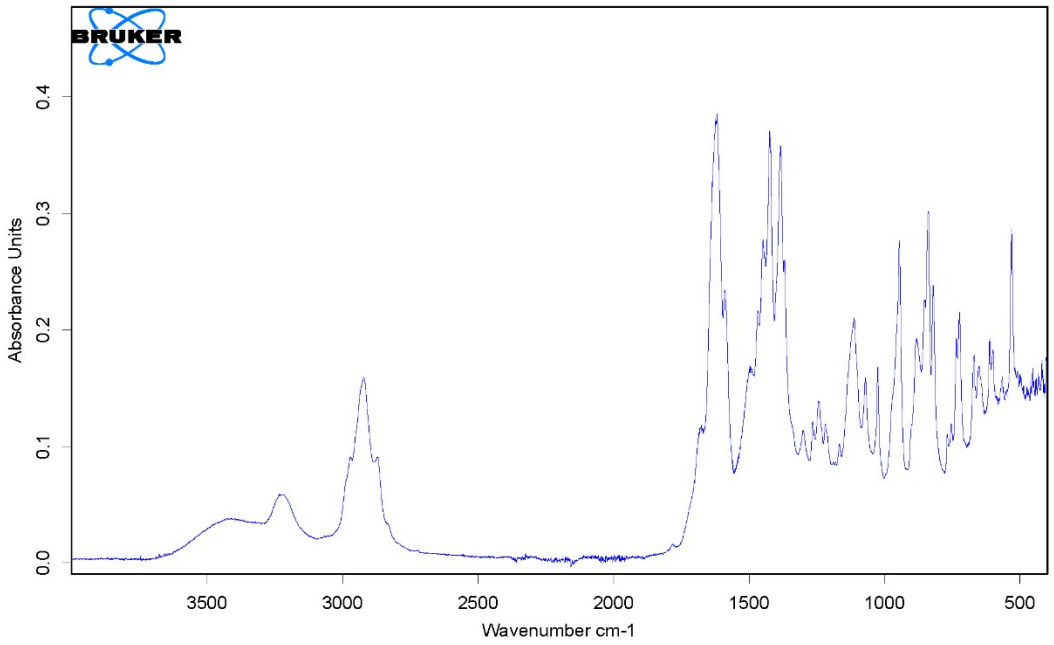

Figure S3.2.3. IR data for tetrazinanone **T2a**

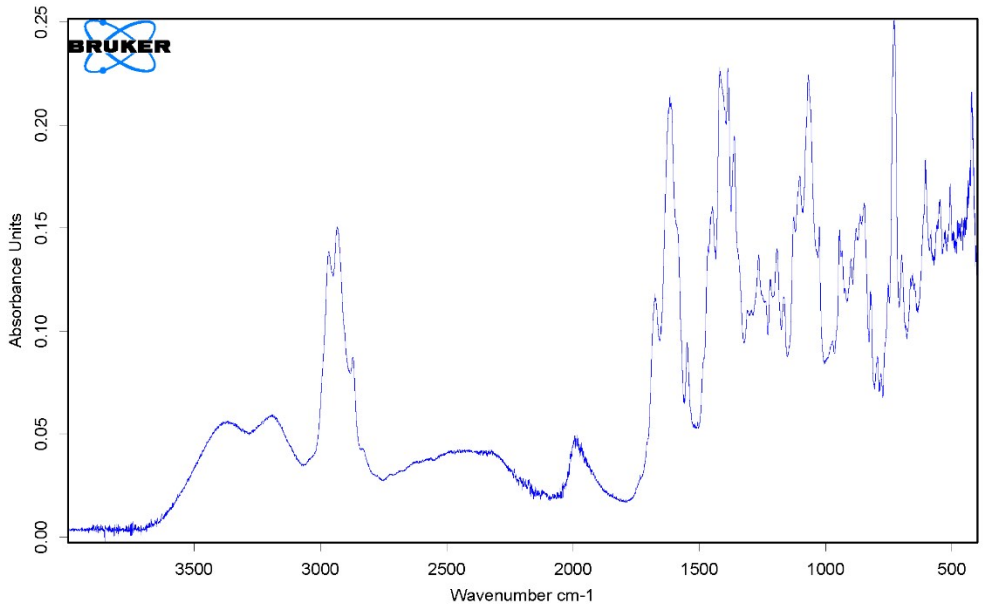

Figure S3.2.4. IR data for tetrazinanone **T1b**

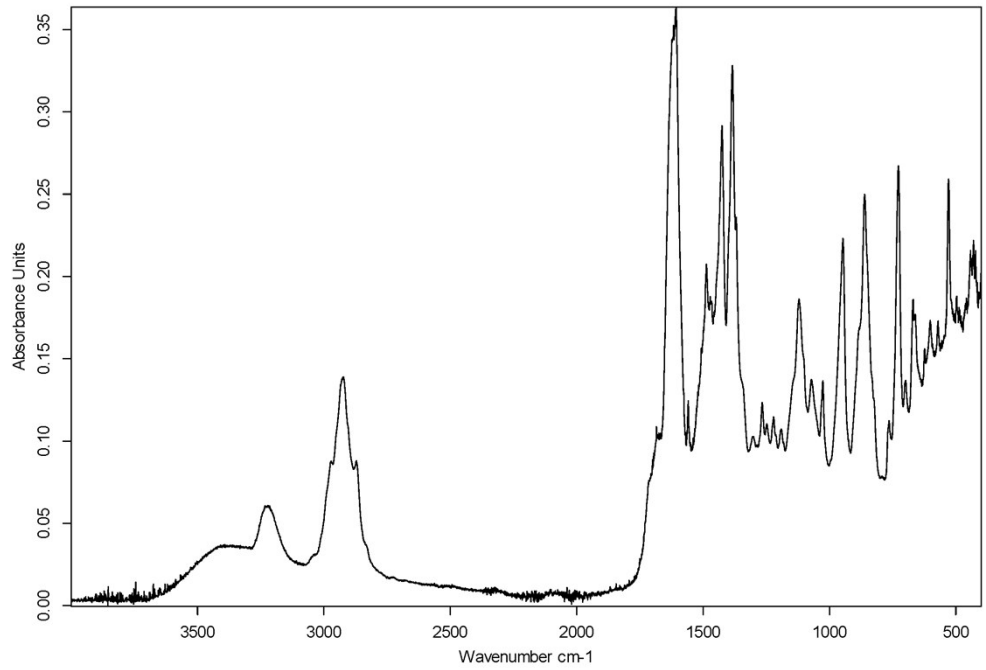

Figure S3.2.5. IR data for tetrazinanone **T2b**

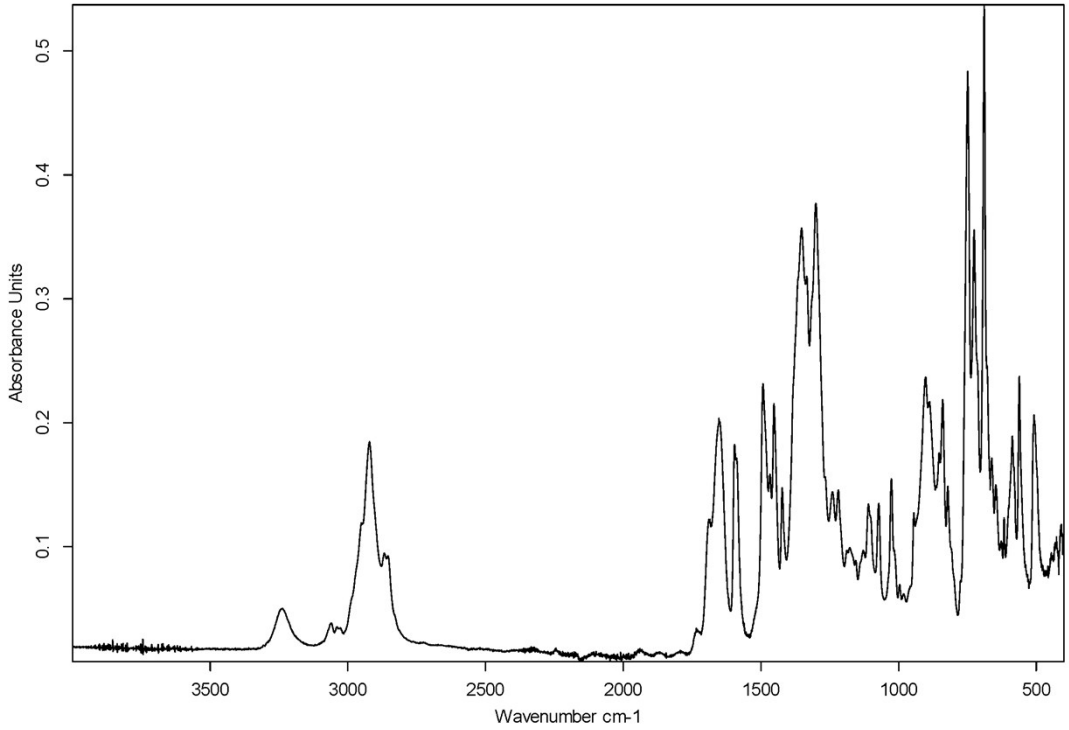

Figure S3.2.6. IR data for tetrazinanone **T1c**

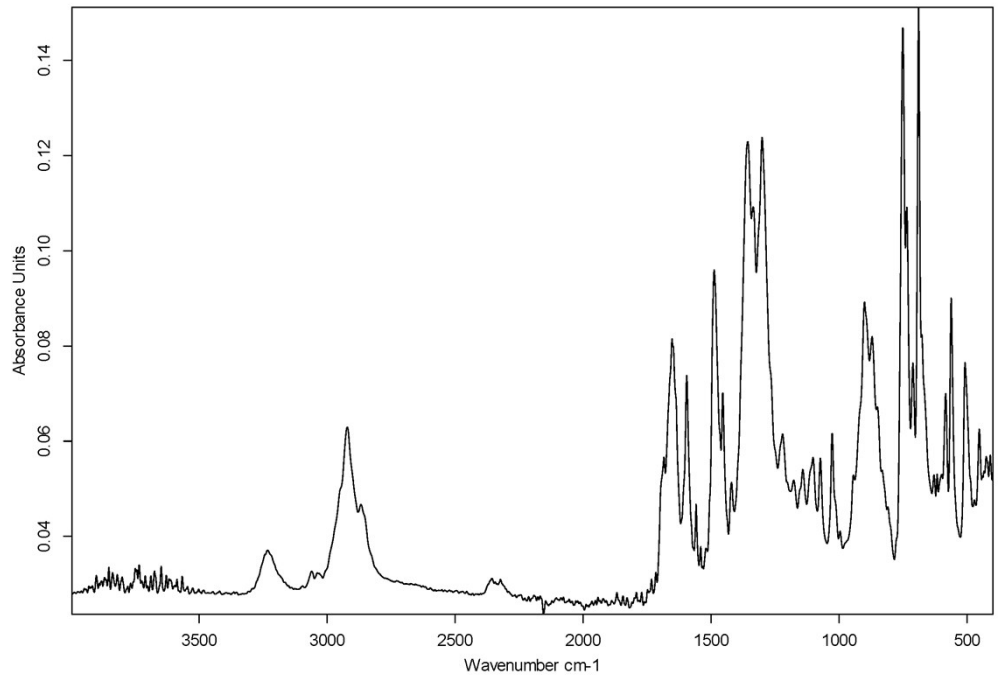

Figure S3.2.7. IR data for tetrazinanone **T2c**

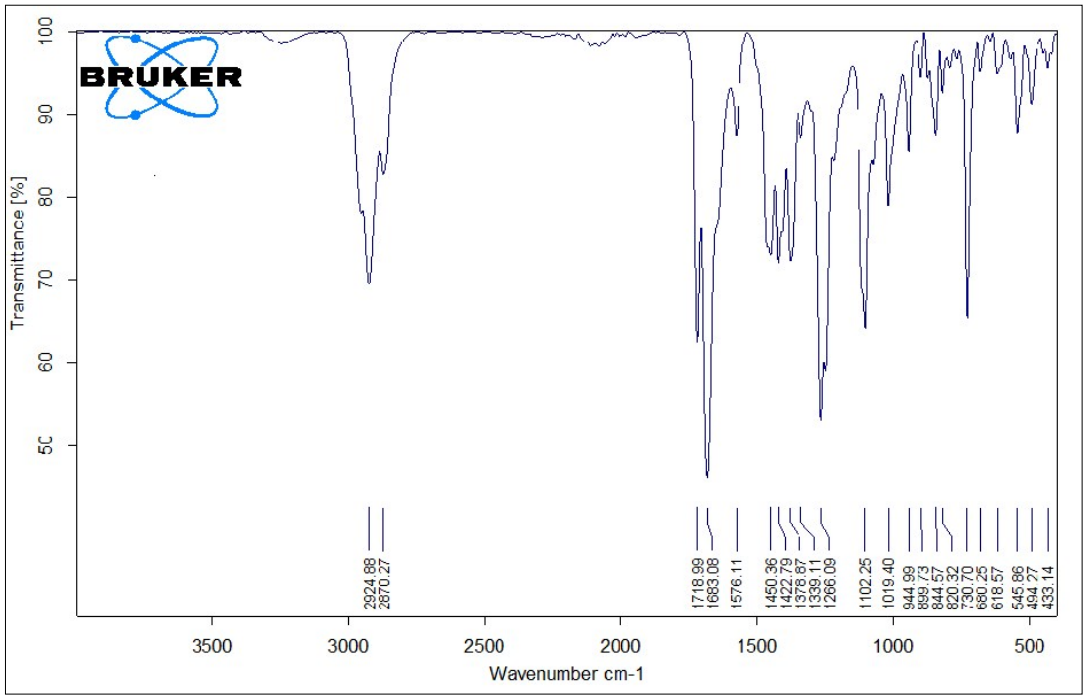

Figure S3.3.9. IR data for the verdazyl radical **1a**

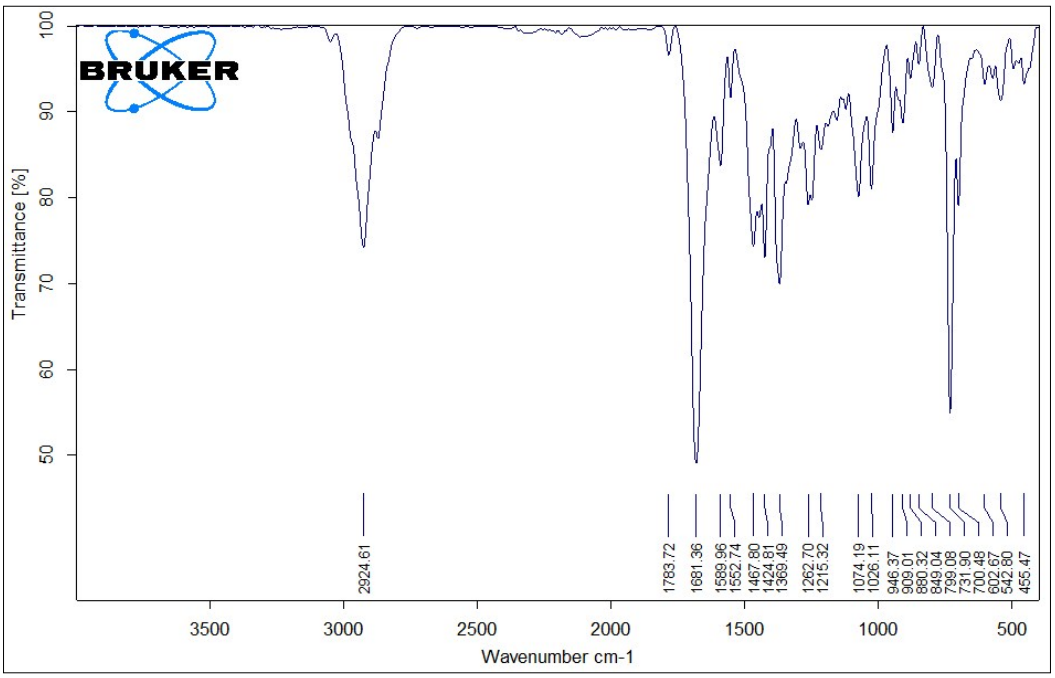

Figure S3.3.10. IR data for the verdazyl radicals **2a**

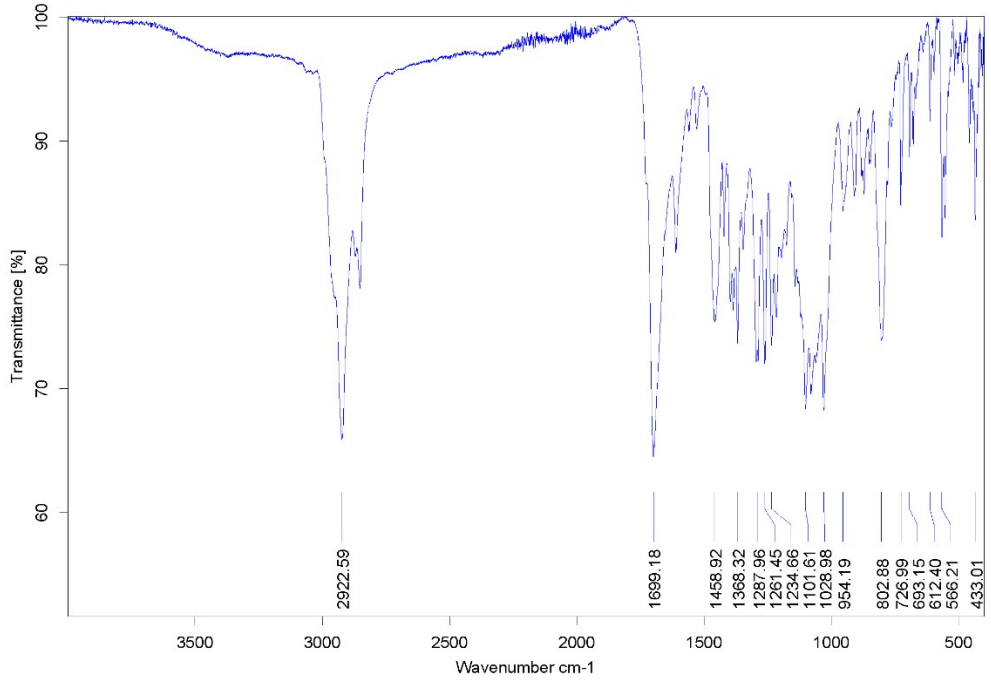

Figure S3.3.11. IR data for the Cu(II) complex **3b**

S3.3 UV-Vis spectroscopy data

The UV-Vis spectra show a broad band between 310-440 nm, which is typical for verdazyl radicals, most likely corresponding to internal π-π* transitions. This band shows a bathochromic shift from 350 nm, for the dimethyl substituted (**1a** and **2a**), to about 360 nm for the diphenyl substituted (**1c** and **2c**), to 410 nm for the diisopropyl substituted (**1b** and **2b**) verdazyls. These values are in accordance with the values found in the literature for similar compounds.[15] In the case of the verdazyl radical **1a** which is complexed with benzoquinone, a larger bathochromic shift is noticeable.

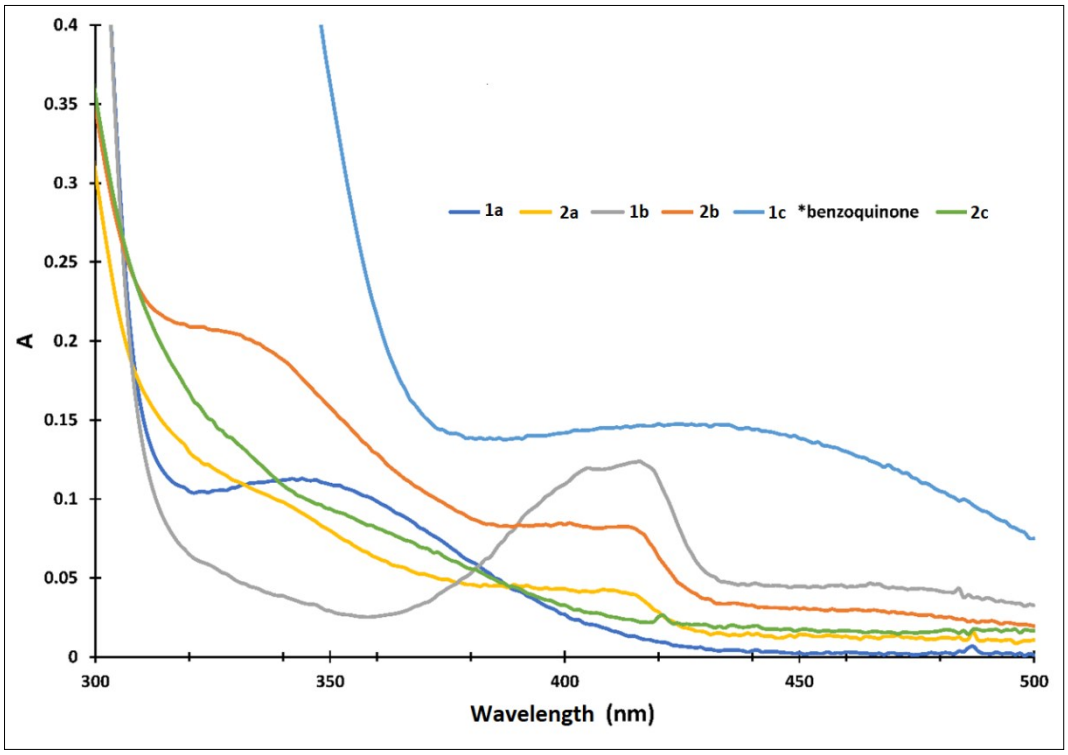

Figure S3.4 UV-Vis spectra for verdazyl radicals **1a** -**1c** and **2a** – **2c**.

S 3.4 HRMS Data

XMASS Mass Analysis for /Data/EIF/WOLL1809_ESI/1/pdata/1/massanal.res:
XMASS Mass Analysis Constraints

Ion mass = 465.2108190

Charge = +1

#	C	H	N	O	Na	mass	DBE	error
*** Mass Analysis for mass 465.2108190								
1	**23**	**30**	**4**	**5**	**1**	**465.2108412**	10.5	2.218e-05
2	22	31	3	8	0	465.2105664	9.0	2.526e-04
3	21	25	10	3	0	465.2105611	14.5	2.579e-04
4	23	27	7	4	0	465.2119038	14.0	1.085e-03
5	21	28	7	4	1	465.2094985	11.0	1.320e-03
6	24	26	8	1	1	465.2121786	15.5	1.360e-03
7	25	32	1	6	1	465.2121839	10.0	1.365e-03
8	20	29	6	7	0	465.2092237	9.5	1.595e-03
9	34	27	1	1	0	465.2087159	22.0	2.103e-03
10	25	29	4	5	0	465.2132465	13.5	2.427e-03

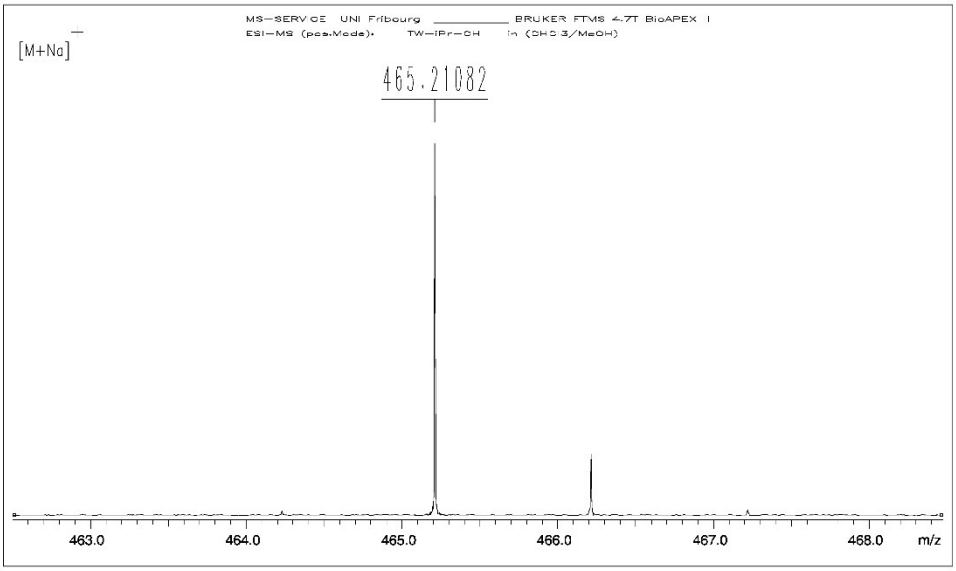

Figure S3.3.1. HRMS data for **Boc2.**

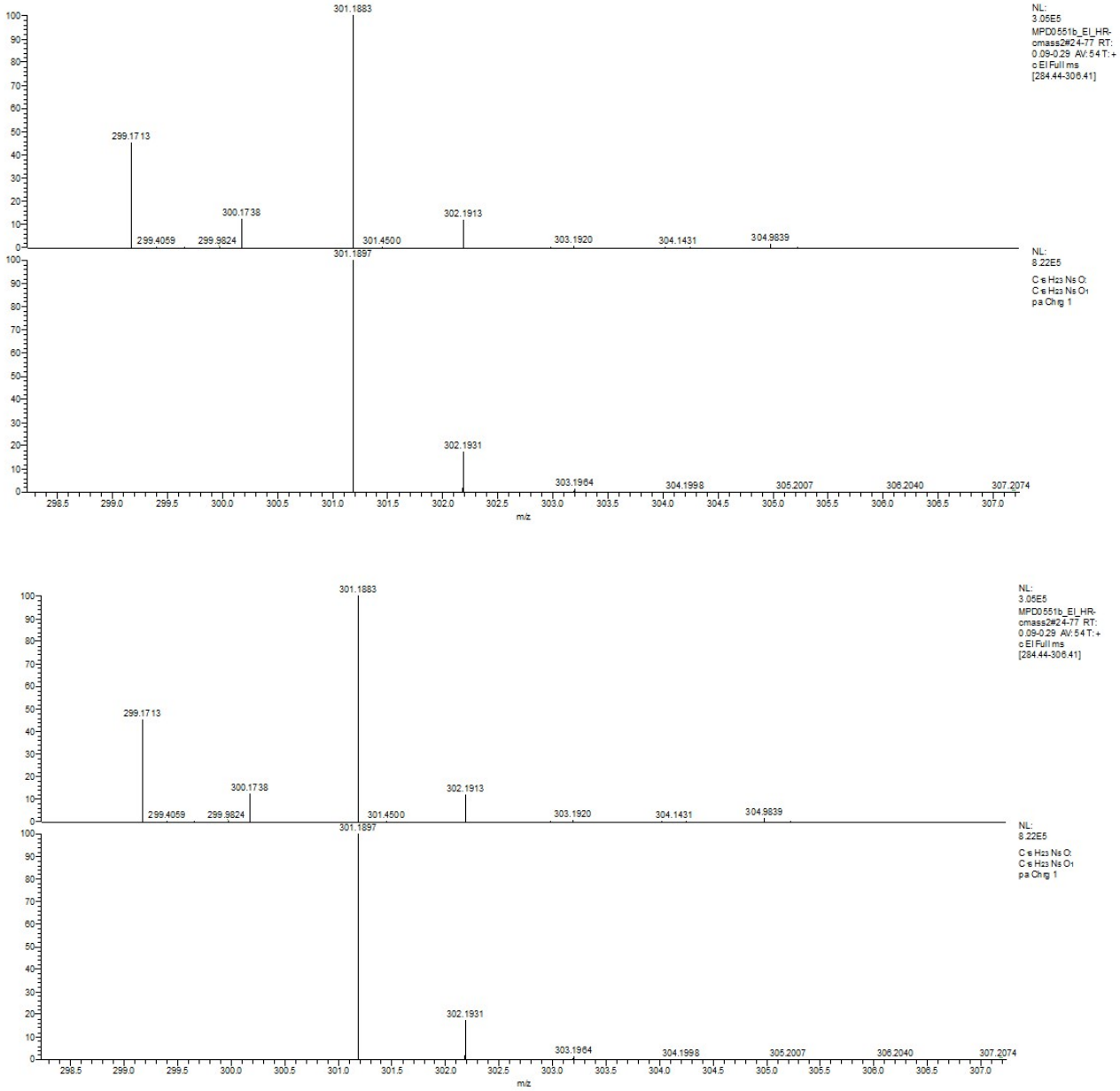

Figure S3.3.2. HRMS data for **T1a** (top) and **T2a** (bottom). For $[M]^+$ $C_{16}H_{23}N_5O$ required 301.1903; Found 301.1883.

XMASS Mass Analysis for /Data/UNI_FR/WOLL1787_ESI/5/pdata/1/massanal.res:
XMASS Mass Analysis Constraints

Ion mass = 358.2600630

Charge = +1

#	C	H	N	O	mass	DBE	error
*** Mass Analysis for mass 358.2600630							
1	**20**	**32**	**5**	**1**	**358.2601371**	7.5	7.410e-05
2	19	36	1	5	358.2587997	2.5	1.263e-03
3	22	34	2	2	358.2614798	7.0	1.417e-03
4	17	34	4	4	358.2574570	3.0	2.606e-03
5	15	32	7	3	358.2561143	3.5	3.949e-03
6	11	34	8	5	358.2646677	-1.0	4.605e-03
7	14	36	3	7	358.2547769	-1.5	5.286e-03
8	13	30	10	2	358.2547717	4.0	5.291e-03
9	13	36	5	6	358.2660103	-1.5	5.947e-03
10	12	34	6	6	358.2534343	-1.0	6.629e-03

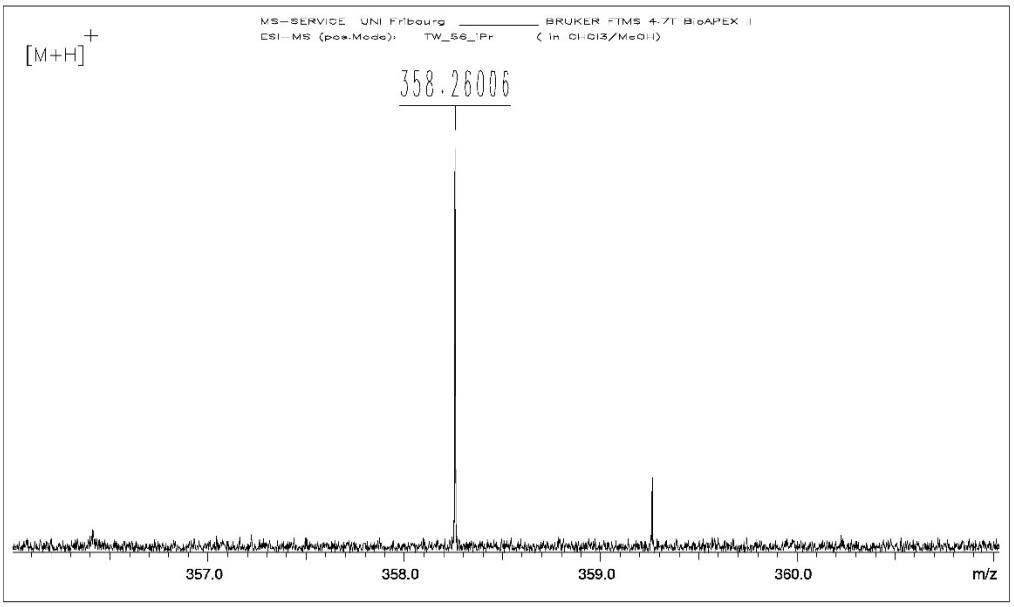

Figure S3.3.3. HRMS data for **T1b.**

XMASS Mass Analysis for /Data/UNI_FR/WOLL1786_ESI/2/pdata/1/massanal.res:
XMASS Mass Analysis Constraints

Ion mass = 358.2603360

Charge = +1

#	C	H	N	O	mass	DBE	error
*** Mass Analysis for mass 358.2603360							
1	**20**	**32**	**5**	**1**	**358.2601371**	7.5	1.989e-04
2	22	34	2	2	358.2614798	7.0	1.144e-03
3	19	36	1	5	358.2587997	2.5	1.536e-03
4	17	34	4	4	358.2574570	3.0	2.879e-03
5	15	32	7	3	358.2561143	3.5	4.222e-03
6	11	34	8	5	358.2646677	-1.0	4.332e-03
7	14	36	3	7	358.2547769	-1.5	5.559e-03
8	13	30	10	2	358.2547717	4.0	5.564e-03
9	13	36	5	6	358.2660103	-1.5	5.674e-03
10	12	34	6	6	358.2534343	-1.0	6.902e-03

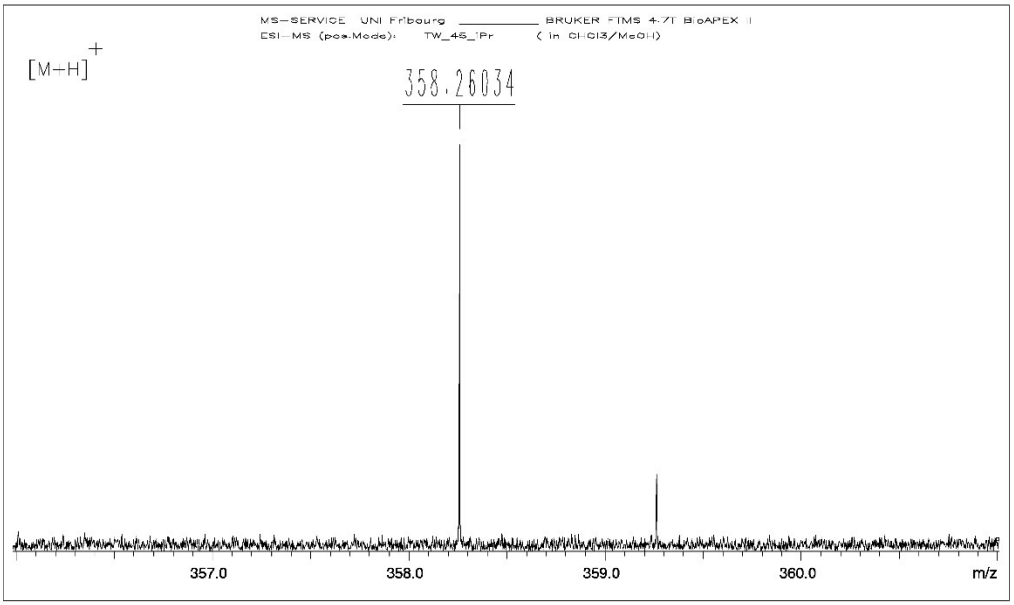

Figure S3.3.4. HRMS data for **T2b.**

XMASS Mass Analysis for /Data/UNI_FR/MAMU2318_ESI/1/pdata/1/massanal.res:
XMASS Mass Analysis Constraints

Ion mass = 426.2290060

Charge = +1

#	C	H	N	O	mass	DBE	error
*** Mass Analysis for mass 426.2290060							
1	**26**	**28**	**5**	**1**	**426.2288370**	15.5	1.690e-04
2	12	30	10	7	426.2293448	3.0	3.388e-04
3	28	30	2	2	426.2301796	15.0	1.174e-03
4	25	32	1	5	426.2274996	10.5	1.506e-03
5	14	32	7	8	426.2306875	2.5	1.681e-03
6	9	32	9	10	426.2266647	-1.5	2.341e-03
7	23	30	4	4	426.2261569	11.0	2.849e-03
8	16	34	4	9	426.2320301	2.0	3.024e-03
9	21	28	7	3	426.2248142	11.5	4.192e-03
10	17	30	8	5	426.2333675	7.0	4.362e-03

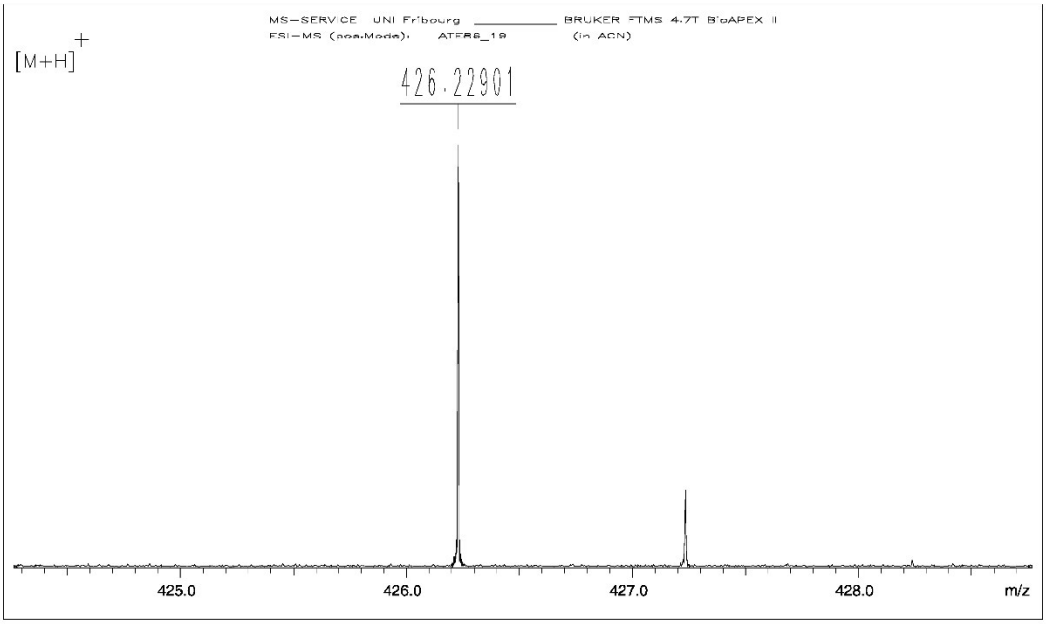

Figure S3.3.5. HRMS data for **T1c.**

Ion mass = 426.2282830

Charge = +1

#	C	H	N	O	mass	DBE	error
*** Mass Analysis for mass 426.2282830							
1	**26**	**28**	**5**	**1**	**426.2288370**	15.5	5.540e-04
2	25	32	1	5	426.2274996	10.5	7.834e-04
3	12	30	10	7	426.2293448	3.0	1.062e-03
4	9	32	9	10	426.2266647	-1.5	1.618e-03
5	28	30	2	2	426.2301796	15.0	1.897e-03
6	23	30	4	4	426.2261569	11.0	2.126e-03
7	14	32	7	8	426.2306875	2.5	2.404e-03
8	21	28	7	3	426.2248142	11.5	3.469e-03
9	16	34	4	9	426.2320301	2.0	3.747e-03
10	20	32	3	7	426.2234768	6.5	4.806e-03

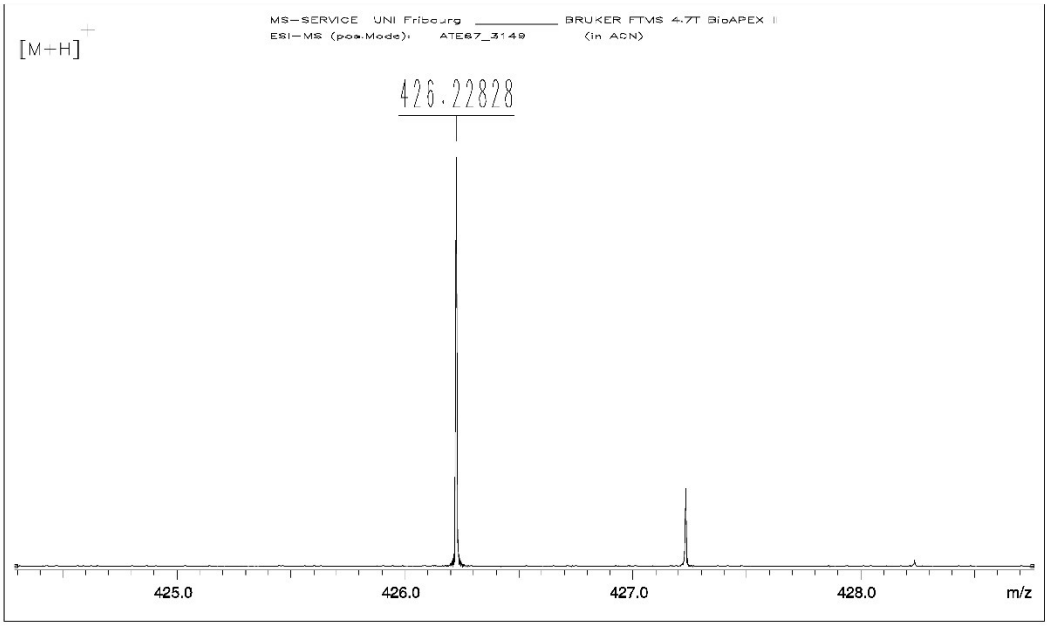

Figure S3.3.6. HRMS data for **T2c.**

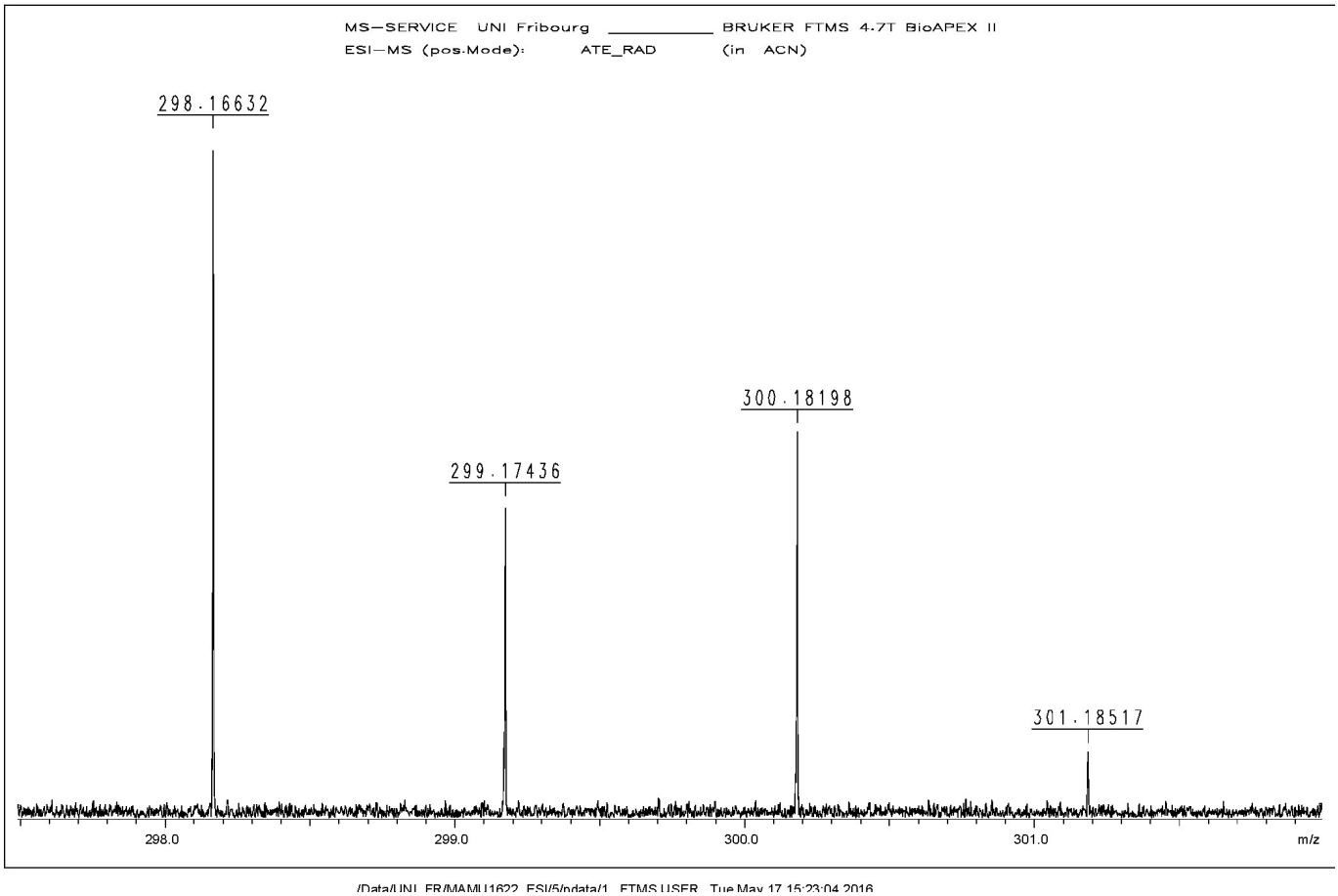

Figure S3.3.7. HRMS data for **1a.**

Ion mass = 298.1660220

Charge = +1

#	C	H	N	O	mass	DBE	error
*** Mass Analysis for mass 298.1660220							
1	**16**	**20**	**5**	**1**	**298.1662367**	9.5	2.147e-04
2	15	24	1	5	298.1648993	4.5	1.123e-03
3	18	22	2	2	298.1675794	9.0	1.557e-03
4	13	22	4	4	298.1635566	5.0	2.465e-03
5	11	20	7	3	298.1622140	5.5	3.808e-03
6	7	22	8	5	298.1707673	1.0	4.745e-03
7	10	24	3	7	298.1608766	0.5	5.145e-03
8	9	18	10	2	298.1608713	6.0	5.151e-03
9	9	24	5	6	298.1721099	0.5	6.088e-03
10	8	22	6	6	298.1595339	1.0	6.488e-03

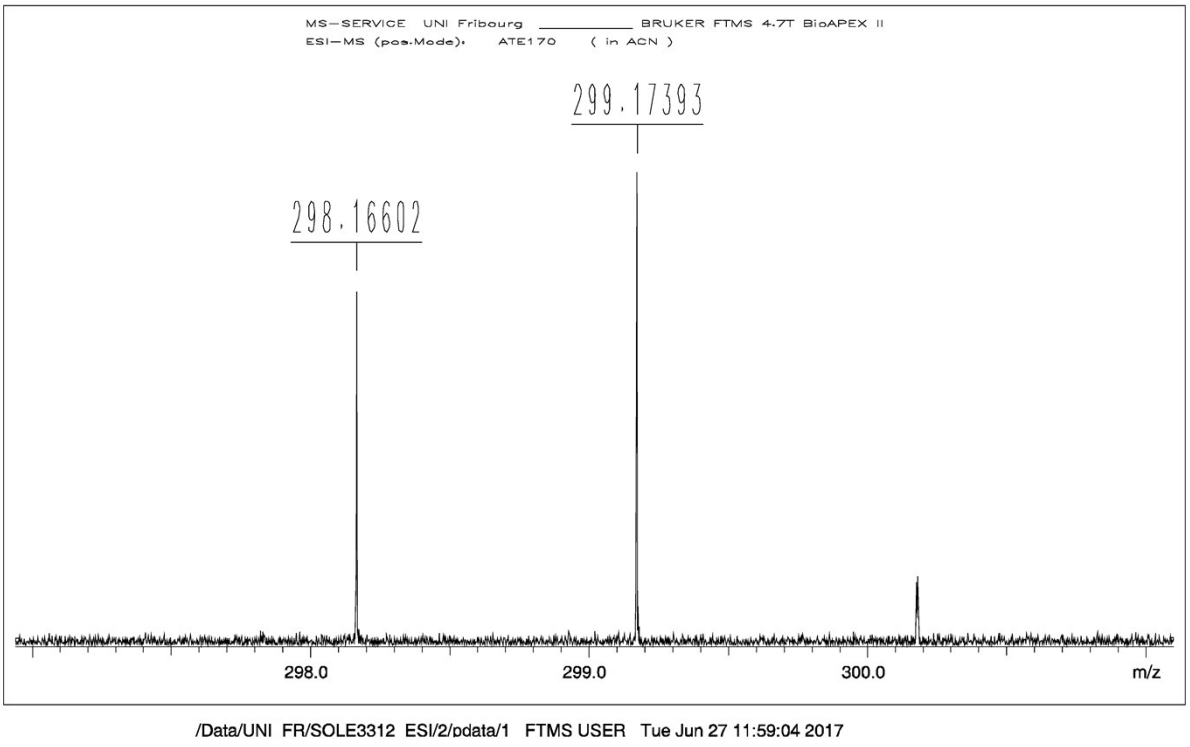

Figure S3.3.8. HRMS data for **2a.**

Ion mass = 355.2360750

Charge = +1

#	C	H	N	O	mass	DBE	error
*** Mass Analysis for mass 355.2360750							
1	**20**	**29**	**5**	**1**	**355.2366620**	9.0	5.870e-04
2	19	33	1	5	355.2353246	4.0	7.504e-04
3	22	31	2	2	355.2380047	8.5	1.930e-03
4	17	31	4	4	355.2339819	4.5	2.093e-03
5	15	29	7	3	355.2326393	5.0	3.436e-03
6	14	33	3	7	355.2313018	0.0	4.773e-03
7	13	27	10	2	355.2312966	5.5	4.778e-03
8	11	31	8	5	355.2411926	0.5	5.118e-03
9	12	31	6	6	355.2299592	0.5	6.116e-03
10	13	33	5	6	355.2425352	0.0	6.460e-03

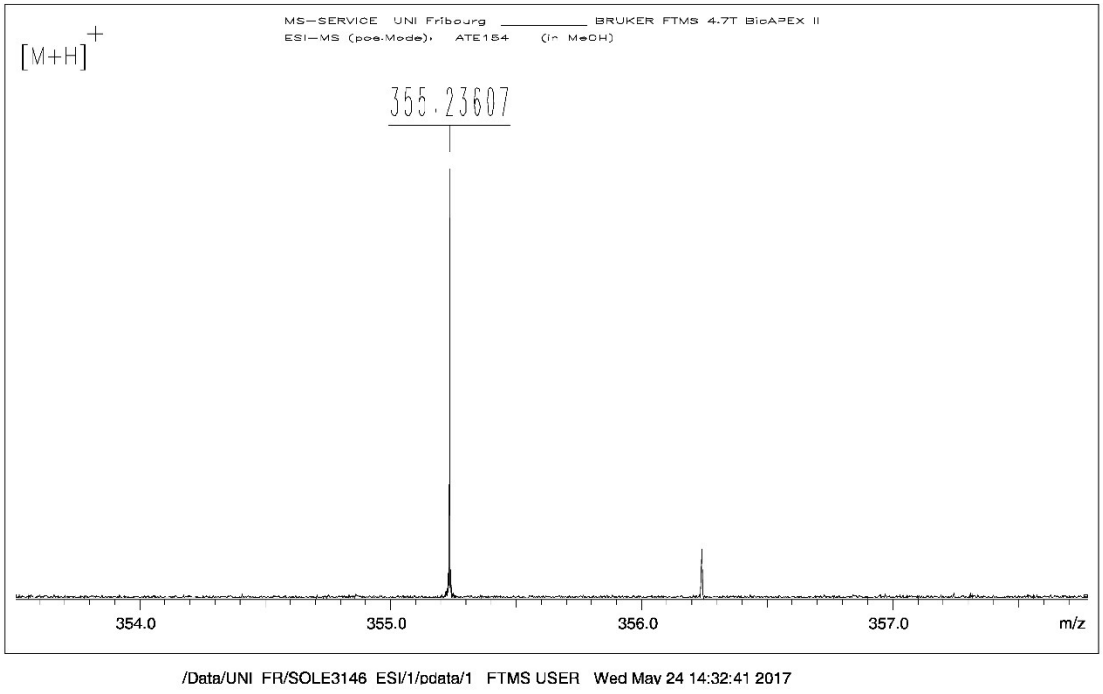

Figure S3.3.9. HRMS data for **1b.**

Ion mass = 355.2368650

Charge = +1

#	C	H	N	O	mass	DBE	error
*** Mass Analysis for mass 355.2368650							
1	**20**	**29**	**5**	**1**	**355.2366620**	9.0	2.030e-04
2	22	31	2	2	355.2380047	8.5	1.140e-03
3	19	33	1	5	355.2353246	4.0	1.540e-03
4	17	31	4	4	355.2339819	4.5	2.883e-03
5	15	29	7	3	355.2326393	5.0	4.226e-03
6	11	31	8	5	355.2411926	0.5	4.328e-03
7	14	33	3	7	355.2313018	0.0	5.563e-03
8	13	27	10	2	355.2312966	5.5	5.568e-03
9	13	33	5	6	355.2425352	0.0	5.670e-03
10	12	31	6	6	355.2299592	0.5	6.906e-03

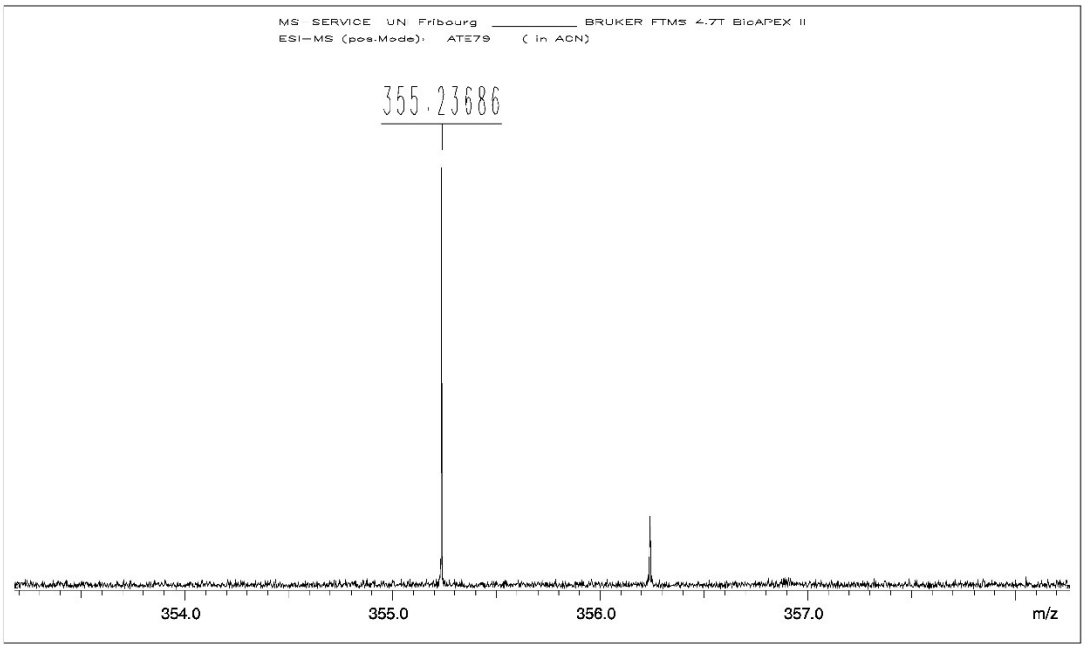

Figure S3.3.10. HRMS data for **2b.**

Ion mass = 530.2188050

Charge = +1

#	C	H	N	O	mass	DBE	error
*** Mass Analysis for mass 530.2188050							
1	**32**	**28**	**5**	**3**	**530.2186662**	21.5	1.388e-04
2	18	30	10	9	530.2191740	9.0	3.690e-04
3	34	30	2	4	530.2200089	21.0	1.204e-03
4	31	32	1	7	530.2173288	16.5	1.476e-03
5	30	26	8	2	530.2173235	22.0	1.481e-03
6	20	32	7	10	530.2205167	8.5	1.712e-03
7	29	30	4	6	530.2159861	17.0	2.819e-03
8	27	28	7	5	530.2146435	17.5	4.162e-03
9	23	30	8	7	530.2231968	13.0	4.392e-03
10	26	32	3	9	530.2133061	12.5	5.499e-03

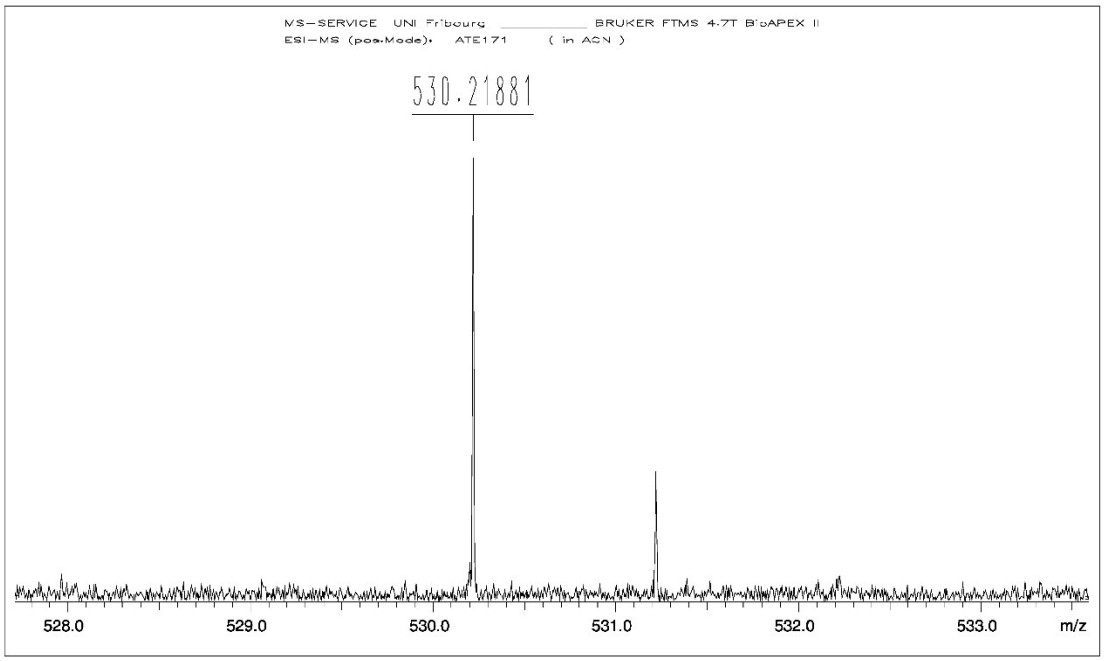

Figure S3.3.11. HRMS data for **1c*benzoquinone.**

Ion mass = 423.2048840

Charge = +1

#	C	H	N	O	mass	DBE	error
*** Mass Analysis for mass 423.2048840							
1	**26**	**25**	**5**	**1**	**423.2053619**	17.0	4.779e-04
2	25	29	1	5	423.2040245	12.0	8.595e-04
3	12	27	10	7	423.2058697	4.5	9.857e-04
4	9	29	9	10	423.2031896	0.0	1.694e-03
5	28	27	2	2	423.2067045	16.5	1.821e-03
6	23	27	4	4	423.2026818	12.5	2.202e-03
7	14	29	7	8	423.2072124	4.0	2.328e-03
8	21	25	7	3	423.2013391	13.0	3.545e-03
9	16	31	4	9	423.2085550	3.5	3.671e-03
10	20	29	3	7	423.2000017	8.0	4.882e-03

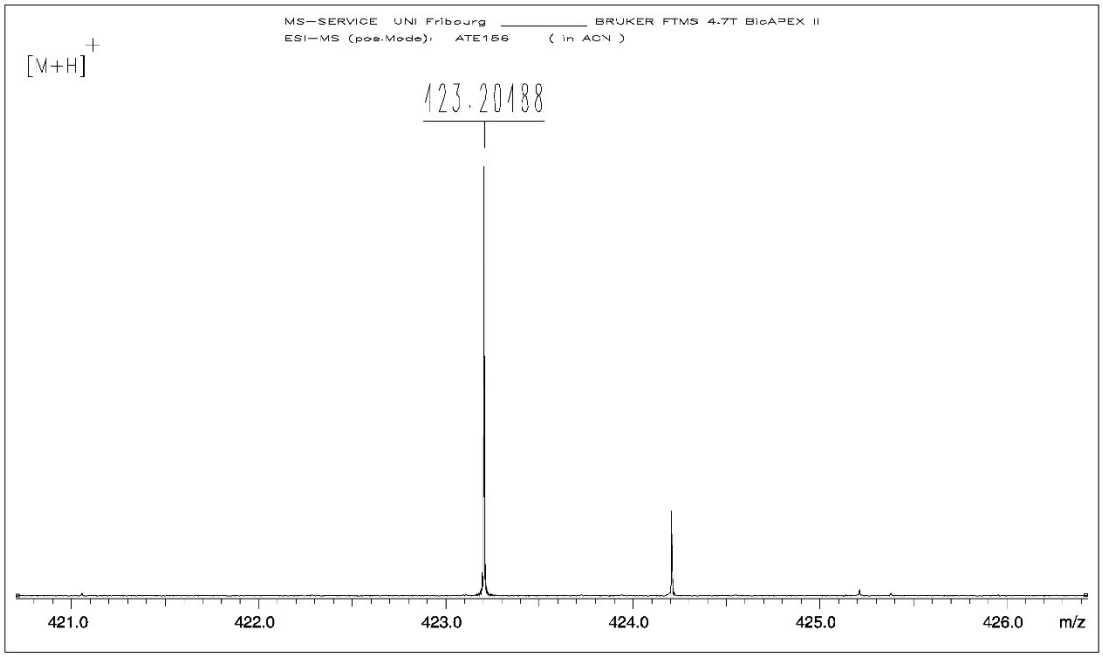

Figure S3.3.12. HRMS data for **2c**

S 3.5 EPR Data

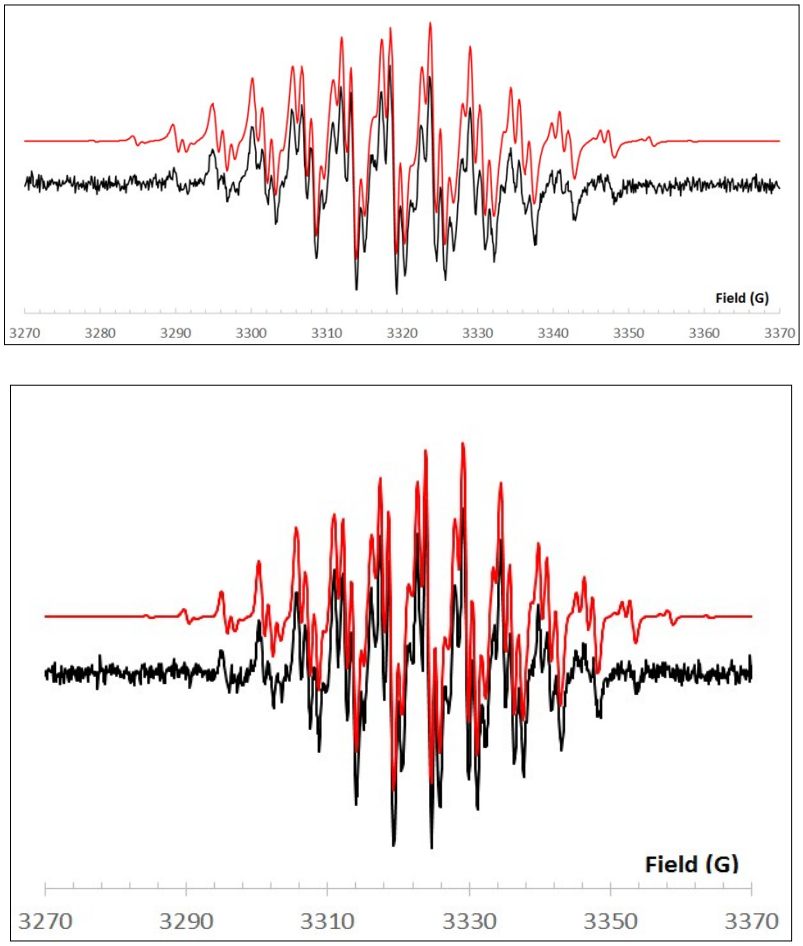

Figure S3.4 EPR spectra of 5,6-Me **1a** (top) and 4,5-Me **2a** (bottom) at 298 K in DCM. Both simulated spectra based on a_N = 6.45 G (2N), a_N = 5.15 G (2N), and a_H = 5.45 G (6H). The EPR spectra of **1a** and **2a** comprise a complex multiplet that can be attributed to the hyperfine coupling of the radical coupled to the four verdazyl nitrogen atoms, plus some additional super-hyperfine coupling which can be attributed to the two CH_3 hydrogen atoms of the dimethyl substituents.

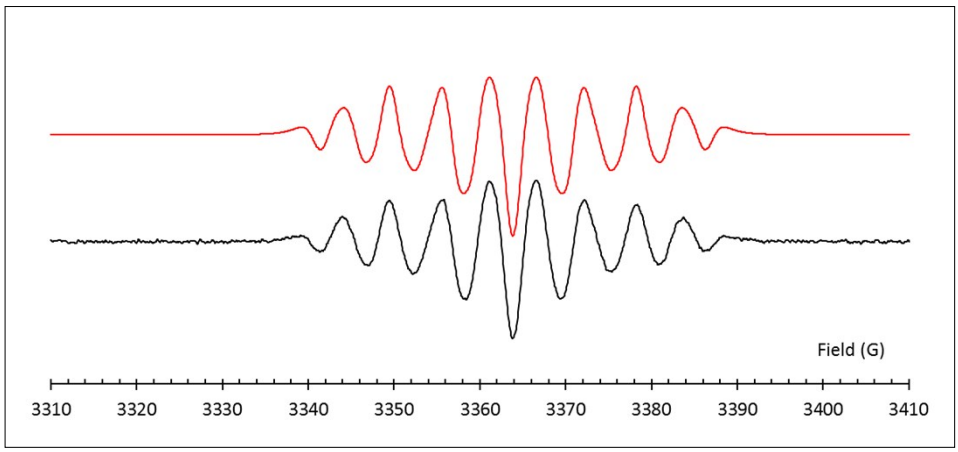

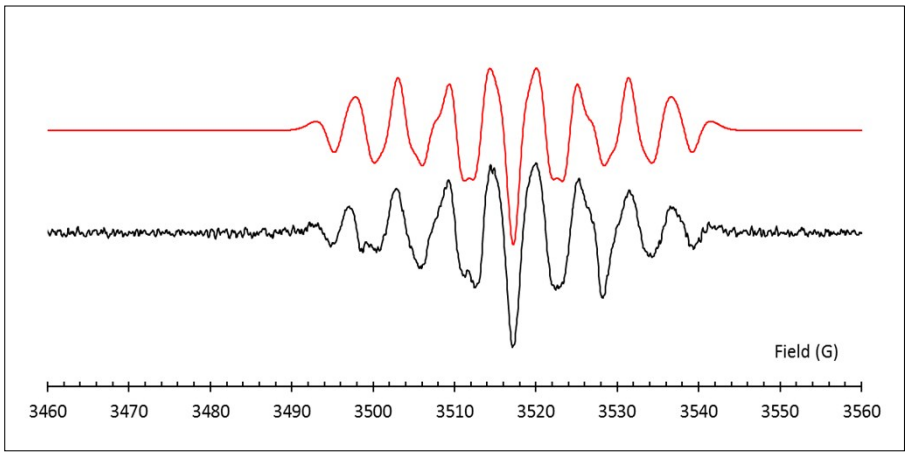

Figure S3.5 Second derivative EPR spectra of 5,6-Ph **1c** (top) and 4,5-Ph **2c**(bottom) at 298 K in DCM. Experimental spectra in black and simulations in red. For **1c** the spectrum was simulated using a_N = 6.39 G (2N), a_N = 4.78 G (2N), and a_H = 0.61 G (4H),* linewidth 1.85 G_{pp}. [Hyperfine coupling to H atoms was less than the inherent linewidth and unresolved. For **2c** the spectrum was simulated using a_N = 6.35 G (2N), a_N = 4.60 G (2N), and a_H = 0.57 G (4H),* linewidth 1.4 G_{pp}. The values quoted are estimated based on the best fit to the line shape].

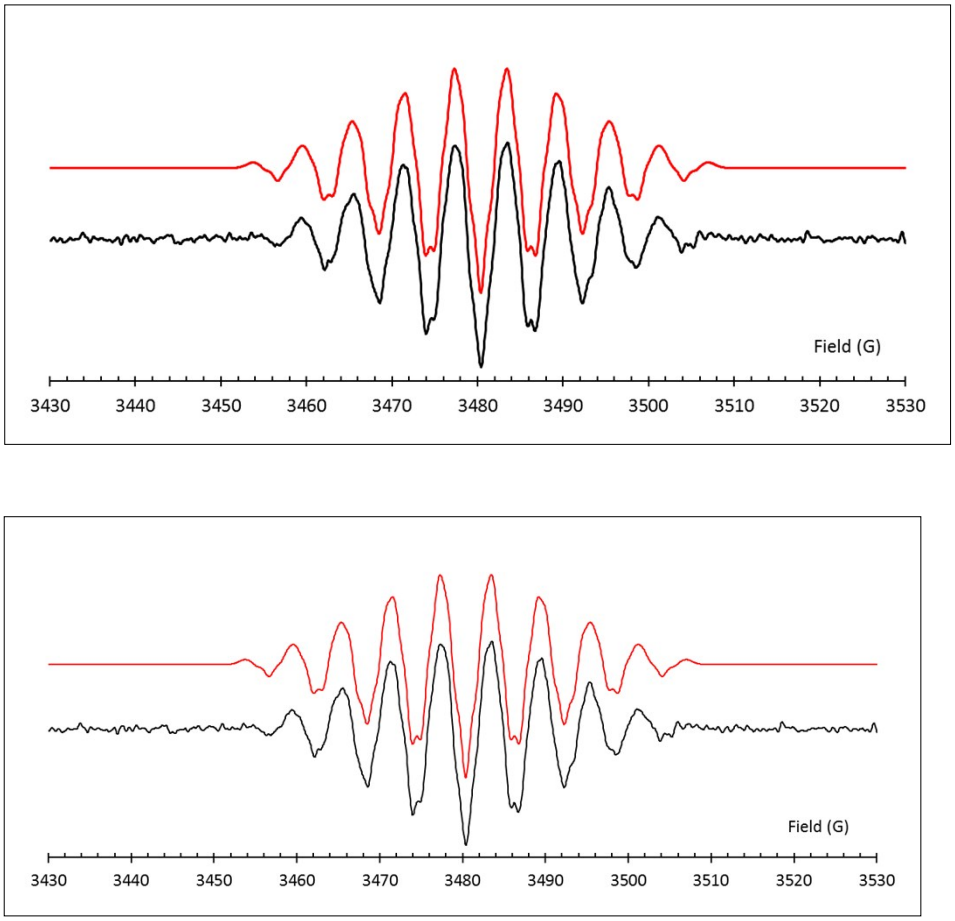

Figure S3.6 Second derivative EPR spectra of 5,6-iPr **1b** (top) and 4,5-iPr **2b**(bottom) at 298 K in DCM. Experimental spectra in black and simulations in red. Both spectra were simulated using a_N = 6.48 G (2N), a_N = 5.47 G (2N), and a_H = 1.47 G (2H),* linewidth 1.0 G_{pp}.

S4. Computational Studies

DFT and TD-DFT calculations were undertaken on radicals **1a** and **2a** based on a geometry-optimised UB3LYP-6311G** structure using an open shell doublet configuration which afforded no imaginary frequencies consistent with an energy minimum. All calculations were performed within Jaguar 9.0. The nature of the singly occupied molecular orbital and the total spin density distribution is shown in Figure S4 and reveal the unpaired electron density in both cases is primarily located on the verdazyl moiety. For radical **1a** significant (> ±3%) Mulliken atomic spin densities revealed comprised a negative spin density at the C-centre (-13.7%),* 39.4 and 38.4% on the N atoms adjacent to the pyridyl ring and 19.4 and 19.6% adjacent to the carbonyl. For radical **2a** the corresponding spin densities are: C -13.7%, N 39.2 and 38.6%, N 19.6 and 19.5% respectively. The presence of the pyridyl ring clearly leads to a breaking of the symmetry and a slight asymmetry in the spin distribution within both molecules. Nevertheless, each can be considered as having two pairs of near-equivalent N atoms with each pair bearing ca. 39% and 19.5% spin density each. This is consistent with the experimental EPR spectra which reveal coupling to two sets of two chemically distinct ^{14}N nuclei (I = 1), with additional hyperfine coupling to the methyl-H atoms arising through hyper-conjugation effects. For information: The different energy of electron-electron repulsions between 'spin-up' and 'spin-up' ('α' electrons) is less than the electron-electron repulsion between 'spin up' and 'spin down' ('β' electrons) electrons due to quantum effects. [Consider Hund's rules of maximum multiplicity which we apply to transition metal ion configurations; electrons prefer to be placed in separate orbitals co-parallel (because the anti-parallel configuration is higher in energy)]. With an odd number of electrons the energy of the α-spins and β-spins are not quite the same since the α-spins are repelled by n β-spins whereas the β-spins are repelled by (n+1) α-spins. Since $H\psi = E\psi$ then the difference in energies leads to wavefunctions for the α-spins (ψ_α) which are not the same as ψ_β. Reality is that ψ_β tries to avoid regions where the extra α-electron is. Therefore, there tends to be slightly more than 100% positive (α) spin density and a small 'negative' spin density in regions where the α-spin density is nodal.

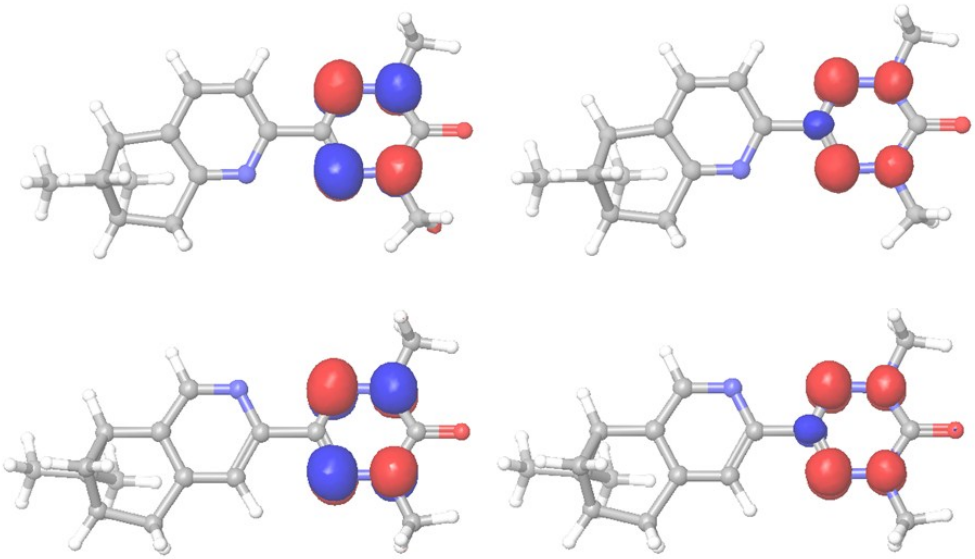

Figure S4. (left) Singly-occupied molecular orbitals for radical **1a** (top) and **2a** (bottom); (right) total spin density distribution for **Ia** (top) and **2a** (bottom) (red = positive spin density, blue= negative spin density)

S5. References

[1] A.L. Sauers, D.M. Ho and S. Bernhard, *J. Org. Chem.*, 2004, **69**, 8910 – 8915.

[2] E.D. Mihelich and D.J. Eickhoff, *J. Org. Chem.*, 1983, **48**, 4135 – 4137.

[3] R. Calabretta, C. Gallina and C. Giordano, *Synthesis*, 1991, 536 – 539.

[4] J. Shao, X. Liu, K. Shu, P. Tang, J. Luo, W. Chen and Y. Yu, *Org. Lett*., 2015, **17**, 4502 – 4505.

[5] D. Matuschek, S. Eusterwiemann, L. Stegemann, C. Doerenkamp, B. Wibbeling, C.G. Daniliuc, N.L. Doltsinis, C.A. Strassert, H. Eckert and A. Studer, *Chem. Sci.*, 2015, **6**, 4712 – 4716.

[6] E.C. Pare, D.J. Brook, A. Brieger, M. Badik and M. Schinke, *Org. Biomol. Chem.*, 2005, **3**, 4258 – 4261.

[7] D.R. Duling, *J. Magn. Reson.*, 1994, **B104**, 105 – 110.

[8] A.D. Bochevarov, E. Harder, T.F. Hughes, J.R. Greenwood, D.A. Braden, D.M. Philipp, D. Rinaldo, M.D. Halls, J. Zhang and R.A. Friesner, *Int. J. Quantum Chem.*, 2013, **113**, 2110 – 2142.

[9] C.L. Barr, P.A. Chase, R.G. hicks, M.T. Lemaire and C.L. Stevens, *J. Org. Chem.*, 1999, **64**, 8893 – 8897.

[10] Y. Masuda, M. Kuratsu, S. Suzuki, M. Kozaki, D. Shiomi, K. Sato, T. Takui, K. Okada, *Polyhedron*, 2009, **28**, 1950 – 1954.

[11] C. W. Johnston, S. D. J. McKinnon, B. O. Patrick, R. G. Hicks, *Dalton Trans.*, 2013, **42**, 16829–16836.

[12] J. Cosier and A.M. Glazer, *J. Appl. Crystallogr.*, 1986, **19**, 105 – 107.

[13] E. Blanc, D. Schwarzenbach and H.D. Flack, *J. Appl. Crystallogr*., 1991, **24**, 1035 – 1041.

[14] G. M. Sheldrick, *Acta Crystallogr*., 2015, **C71**, 3 – 8.

[15] a) D. J. Brook, S. Fornell, J. E. Stevens, B. Noll, T. H. Koch, W. Eisfeld, *Inorg. Chem*. 2000, **39**, 562–567. b) J. B. Gilroy, S. D. J. McKinnon, P. Kennepohl, M. S. Zsombor, M. J. Ferguson, L. K. Thompson, R. G. Hicks, *J. Org. Chem*. 2007, **72**, 8062–8069.